The injury response of aged tendons after induced knockdown of decorin and biglycan during the proliferative and remodeling phases of healing

Christelle Darrieutort-Laffite[1,2], Ashley K. Fung[1], Stephanie N. Weiss[1], Courtney A. Nuss[1], David E. Birk[3], Louis J. Soslowsky[1]
[1] McKay Orthopaedic Research Laboratory, University of Pennsylvania, Philadelphia, PA, [2]Rheumatology Department, Nantes University Hospital, France, [3]Department of Molecular Pharmacology and Physiology, University of South Florida, Tampa, FL
Christelle.Darrieutort-Laffite@pennmedicine.upenn.edu

Disclosures: Christelle Darrieutort-Laffite (N), Ashley K. Fung (N), Stephanie N. Weiss (N), Courtney A. Nuss (N), Louis J. Soslowsky (N)

INTRODUCTION: Tendon injuries are a common clinical problem and are associated with significant pain and disability, impacting quality of life and professional activities, resulting in a significant burden on the health care system. Interactions involving small leucine-rich proteoglycans (SLRPs) and other extracellular matrix molecules are central to the regulation of tendon assembly, as well as in the establishment of tendon mechanical function. Previous studies using conventional biglycan and decorin knockout mice showed that the absence of biglycan impaired initial tendon healing following injury while the absence of decorin impaired late tendon healing[1]. However, these studies were not designed to assess the role of decorin and biglycan in an otherwise normal matrix or at specific times of healing. Therefore, the objective of this study was to determine the specific roles of decorin and biglycan in the early and late phases of tendon healing using inducible knockdown mice by analyzing the effects of their knockdown (decorin, biglycan or both) on tendon morphology, collagen architecture and gene expression. We hypothesized that knockdown of decorin, biglycan or both would have significant effects on fibril structure and gene expression during re-establishment of tendon architecture after injury.

METHODS: Female wildtype (WT, n=36), *Dcn*$^{flox/flox}$ (I-*Dcn*$^{-/-}$, n=36), *Bgn*$^{flox/flox}$ (I-*Bgn*$^{-/-}$, n=36), and compound *Dcn*$^{flox/flox}$/*Bgn*$^{flox/flox}$ (I-*Dcn*$^{-/-}$/*Bgn*$^{-/-}$, n=36) mice with a tamoxifen (TM) inducible Cre, (B6.129-Gt (ROSA)26Sortm1(cre/ERT2)Tyj/J, Jackson Labs) were used (IACUC approved)[3]. Aged mice (300 days) underwent bilateral patellar tendon injury surgery[1,2]. Following injury, Cre excision of the conditional alleles was induced 5 days (TM5 groups) after the initial inflammatory phase of healing or after 21 days (TM21 groups) during the remodeling phase of healing via two consecutive daily IP injections of tamoxifen (2 mg/40g body weight). In the WT group, mice received TM injections at 300 days and were allocated to the "uninjured control group" (sacrificed 30 days later) or to the "surgery control groups" (sacrificed at 3 or 6 weeks post-injury). Mice from inducible knockdown genotypes were sacrificed at 3 or 6 weeks post-injury for the TM5 groups while mice from the TM21 groups were sacrificed at 6 weeks post-injury. For histology, knees were fixed, decalcified and embedded in paraffin. Ten-µm transverse sections were obtained every 200µm along the injury and stained with Toluidine Blue. The ratio scar tissue area/tendon area was quantified using custom MATLAB software (n=4/group). For transmission electron microscopy (TEM), patellar tendons were fixed, embedded in epon, and sectioned (85 nm sections). Then, sections were stained with 2% aqueous uranyl acetate followed by 1% phosphotungstic acid and imaged (JEOL 1010). Images were captured in the injury region and the diameter of collagen fibrils was measured (n=4/group). Distributions of fibril diameters were compared between groups with a Kolmogorov-Smirnov test. Finally, samples were collected for gene analysis. After sacrifice, patellar tendons were immediately frozen in liquid nitrogen. After crushing, total RNA was extracted using the Direct-zol RNA Microprep kit (Zymo, R2062), and cDNA was synthesized using the High Capacity cDNA RT kit (Thermo). Pre-amplified cDNA was loaded into a Fluidigm 96.96 Dynamic Array and the expression of 96 genes was studied (collagens, non-collagenous matrix components, genes involved in matrix remodeling, cell differentiation and proliferation or inflammation). Resultant cycle threshold (Ct) values were normalized to the invariant controls (Abl1 and Rps17) and expressed as $2^{\Delta Ct}$ (n=4/group). One-way ANOVAs with Tukey post-hoc tests were used for each timepoint to compare the effect of genotype. Significance was set at $p<0.05$.

RESULTS: At 3 weeks post-injury, a larger scar tissue area was measured in I-*Bgn*$^{-/-}$ tendons compared to I-*Dcn*$^{-/-}$ and WT tendons ($p<0.001$, Fig 1) but there was no difference at 6 weeks. The fibril diameter distributions were statistically different between groups at each time point after early or late knockdown of decorin and biglycan after injury (Fig 2). Gene expression of decorin and biglycan was reduced in the I-*Dcn* $^{-/-}$ and the I-*Bgn*$^{-/-}$ tendons, respectively (Fig 3). I-*Dcn* $^{-/-}$, I-*Bgn*$^{-/-}$ and I-*Dcn*$^{-/-}$/*Bgn*$^{-/-}$ tendons had no effect on other SLRP expression (Asporin, Fibromodulin, Lumican, Keratocan) or collagen expression (Col1a1, Col1a2, Col2a1, Col3a1, Col5a1, Col6a1, Col11a1, Col12a1 or Col14a1). I-*Dcn* $^{-/-}$, I-*Bgn*$^{-/-}$ and I-*Dcn*$^{-/-}$/*Bgn*$^{-/-}$ tendons had no effect on expression of remodeling markers (Mmp2, Mmp3, Mmp9, Mmp13, Adamts5, Timp1, Timp3) except for Bmp-1 in I-*Dcn*$^{-/-}$ and I-*Dcn*$^{-/-}$/*Bgn*$^{-/-}$ tendons at 6 weeks post-injury for either induction time point.

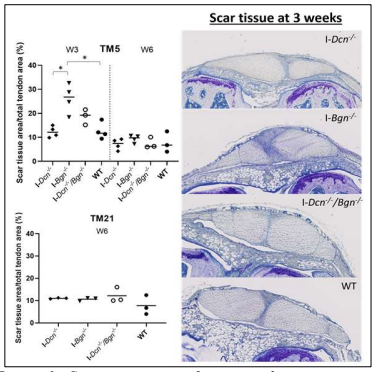

Figure 1. Scar tissue quantification and representative images of TM5-3weeks group. At 3 weeks post-injury, I-Bgn$^{-/-}$ *had a larger scar tissue area than I-Dcn*$^{-/-}$ *and WT tendons but there was no difference at 6 weeks.*

DISCUSSION: We determined the roles of decorin and biglycan during the proliferative and remodeling phases after tendon injury. While early knockdown of biglycan altered early healing as observed in conventional *Bgn*$^{-/-}$ mice, no differences were observed at the later time point suggesting compensatory mechanisms. The knockdown of decorin and/or biglycan impacted post-injury fibrillogenesis demonstrating organizational effects. Previous data showed that knockdown of decorin and biglycan affects collagen fibril structure of mature tendons and this was associated with altered mechanical properties[3]. Future studies will determine the effects on recovery of mechanical properties after injury in these mice.

SIGNIFICANCE/CLINICAL RELEVANCE: The study investigated the role of decorin and biglycan in tendon healing of aged mice and showed a delayed healing in I-*Bgn*$^{-/-}$ tendons when the knockdown was induced during the early phase of healing and an impact on fibrillogenesis after early or late knockdown of decorin, biglycan or both.

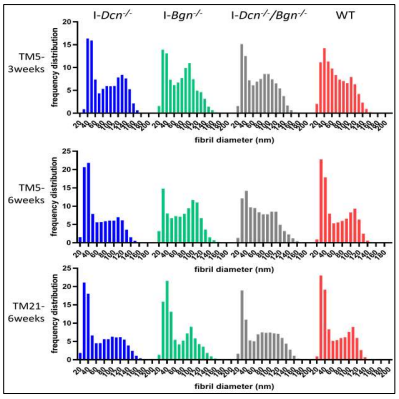

Figure 2. Fibril diameter distributions in percentages within the injury assessed by TEM. Distributions were different between groups at each time point after knockdown of decorin and biglycan.

REFERENCES: [1] Dunkman AA et al., Ann Biomed Eng, 2014, [2] Dunkman et al. Matrix Biol. 35, 2014, [3| Robinson KA et al. Matrix Biol. 64, 2017. **ACKNOWLEDGEMENTS**: This study was funded by NIH/NIAMS (R01AR068057), the Penn Center for Musculoskeletal Disorders (P30AR0696919) and the French Society for Rheumatology (Ref 2645/2019-2020).

Figure 3. Gene expression of decorin and biglycan. Gene expression of decorin was reduced in I-Dcn $^{-/-}$ *and I-Dcn*$^{-/-}$*/Bgn*$^{-/-}$ *tendons while biglycan expression was decreased in I-Bgn*$^{-/-}$ *and I-Dcn* $^{-/-}$*/Bgn*$^{-/-}$ *tendons.*
** =p<0.05 compared to the WT group.*

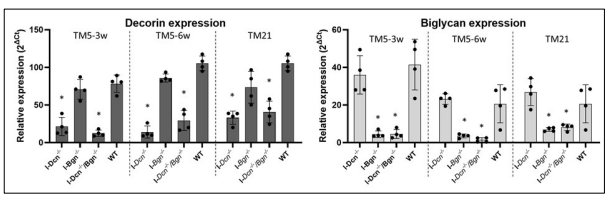

Collagen III Deficiency Alters Mechanical Properties and Decreases Regulation of Fibrillogenesis Following Injury in Female Murine Tendons

Carlson JA[1], Weiss SN[1], Volk SW[2], Soslowsky LJ[1]

[1]McKay Orthopaedic Research Laboratory, University of Pennsylvania, Philadelphia, PA, [2]School of Veterinary Medicine, University of Pennsylvania, Philadelphia, PA

Disclosures: Carlson JA (N), Weiss SN(N), Volk SW(N), Soslowsky LJ (N)

INTRODUCTION: Patients with vascular Ehlers-Danlos syndrome (*v*EDS), a rare genetic disease caused by *Col3A1* mutations, are well-known for severe vascular complications and early death. However, tendon rupture and dysfunction contribute to patient morbidity[1-4], supporting a critical role of collagen III (Col3) in tendon homeostasis and maintenance. Col3 is essential in homeostasis and healing of other collagen I (Col1)-rich tissues (e.g., skin[5], meniscus[6], and bone[7]) due to its role regulating fibrillogenesis, extracellular matrix (ECM) organization, and the formation of cross-links and scar tissue[5,6]. Therefore, the objective of this study was to define the role of Col3 in both tendon homeostasis and in response to injury, regulating collagen fibril deposition and resultant alterations in tendon mechanics. We hypothesized that a reduction in Col3 would result in a more robust, stiffer provisional matrix early in tendon healing, with smaller diameter fibrils when compared to wild-type tendons.

METHODS: Female wild-type (WT) Balb/cJ and heterozygous ***Col3a1***$^{+/-}$ mice at 30 days of age (n=48) were used (IACUC approved). Injured mice underwent bilateral patellar tendon injury surgery[8] and were sacrificed 1-week (1w) post-injury in the early proliferative phase of healing. Uninjured sex, strain and age-matched mice were also examined. *Transmission Electron Microscopy (TEM):* Tendons for TEM (n=4/group) were fixed *in situ* and processed[10] to analyze fibril structure. *Mechanics:* Patella-patellar tendon-tibia complexes were prepared for mechanical testing (n=12/group)[11]. Tendons were subjected to a viscoelastic testing protocol[10,12] consisting of: 1) preconditioning, 2) stress relaxation at strain levels of 2%, 3% and 4%, 3) a sinusoidal frequency sweep (10 cycles at 0.1, 1, 5, and 10 Hz) at each strain level, 4) return to gauge length, and 5) ramp to failure. *Statistics.* Two-way repeated measures ANOVAs with post-hoc Bonferroni tests were used to assess the effects of genotype, injury and their interaction on quasistatic and viscoelastic properties. Collagen fibril diameter distributions were compared by genotype using Kolmogorov-Smirnov tests. Significance was set at $p \leq 0.05$ (solid lines) and trends at $p \leq 0.1$ (dotted lines).

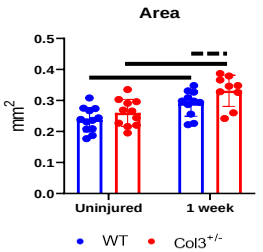

Figure 1. Tendon cross-sectional area was increased post-injury in both genotypes when compared to uninjured tendons.

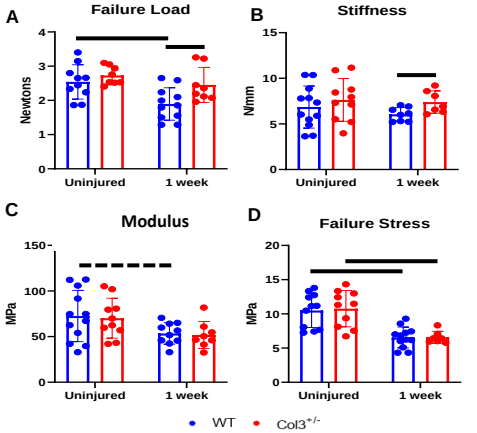

Figure 2. Failure load and stiffness was increased in *Col3a1*$^{+/-}$ tendons 1w post-injury compared to WT. Failure stress was decreased in both genotypes following injury.

RESULTS: Following injury, tendon cross-sectional area was increased in both WT and ***Col3a1***$^{+/-}$ tendons with ***Col3a1***$^{+/-}$ tendons having a larger area than WT tendons (trend) following injury (Fig. 1). ***Col3a1***$^{+/-}$ tendons had increased failure load and stiffness (Fig. 2A,B) 1w post-injury when compared to WT tendons, with no differences in uninjured tissues. Additionally, WT tendons had a lower failure load and modulus (trend) 1w post-injury when compared to uninjured, while there was no effect of injury in ***Col3a1***$^{+/-}$ tendons (Fig. 2A,C). Failure stress (Fig. 2D) was decreased in both genotypes 1w following injury. Additionally, TEM analysis showed a shift to smaller diameter fibrils post-injury in both genotypes (Fig. 3). Finally, distinctly different distributions for WT and ***Col3a1***$^{+/-}$ fibrils post-injury were seen, with ***Col3a1***$^{+/-}$ tendons having a larger population of smaller and larger fibrils, and WT tendons having a less pronounced peak and more flat distribution (Fig. 3).

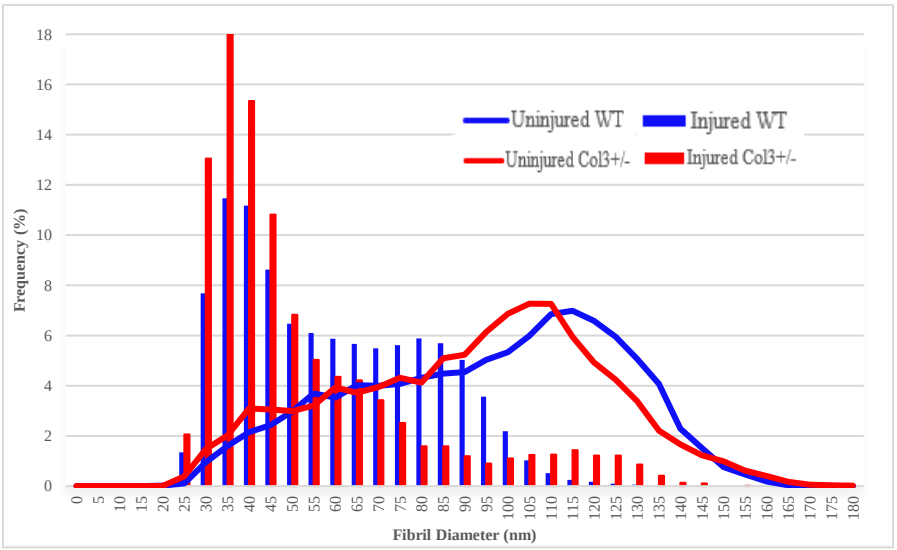

Figure 3. Smaller fibrils were seen in both genotypes following injury. *Col3a1*$^{+/-}$ tendons post-injury had a larger population of smaller fibrils and larger fibrils when compared to WT. Uninjured: line graph, Injured: bar graph.

DISCUSSION: Our study shows that Col3 deficiency alters both mechanical properties and matrix structure 1w post-injury in a murine patellar tendon injury model in novel and previously unexplored ways. Tendon area increases following injury as healing tissue is deposited into the wound site. The trend toward increased area of ***Col3a1***$^{+/-}$ tendons compared to WT tendons post-injury is consistent with an increased deposition of provisional matrix, secondary to increased activation of fibroblasts in ***Col3a1***$^{+/-}$ tendons, as decreased Col3 has been shown to cause increased activation[5]. Decreases in failure stress in both genotypes following injury is due to increases in area without concurrent increases in failure load, indicating poor quality tissue following injury in both genotypes as would be expected 1w post-injury. Additionally, TEM analysis showed a more densely packed provisional matrix with smaller fibrils following injury in ***Col3a1***$^{+/-}$ tendons likely explaining increased stiffness and further indicating a hypersecretory state of myofibroblasts for Col1 post-injury. Lastly, the highly skewed fibril diameter distribution with an extended right tail in ***Col3a1***$^{+/-}$ tendons indicates dysregulation in fibrillogenesis when compared to WT tendons post-injury. An increased population of larger fibrils reveals increased lateralization of fibrils in ***Col3a1***$^{+/-}$ tendons, which is expected as Col3 presence decreases lateral growth during fibrillogenesis[13]. Notably, while ***Col3a1***$^{+/-}$ tendons have increased failure load following injury compared to WT tendons at this time point, the poor quality of healing tissue quantified in this study supports the likelihood of an important role of Col3 in dictating cellular activity and healing potential. Based on these findings, we will examine later time points to understand how fibril growth continues into later stages of healing, along with alterations to the cellular population and activity. Importantly, we will also further evaluate the role of Col3 using a novel conditional Col3 knockdown model to understand the unique temporal role of Col3 throughout healing and more specifically, to rigorously analyze the targeted role of Col3 by evaluating the dose response in an otherwise normal matrix.

SIGNIFICANCE: Col3 is crucial during early wound healing, affecting matrix structure and function, likely influencing long-term healing. Elucidating the mechanistic role of Col3 throughout healing will provide the necessary foundation for developing Col3-inspired therapies that optimize tendon healing and will ultimately have a profound impact on tendon healing, thereby decreasing healthcare expenditures and improving patient quality of life.

REFERENCES: [1] Cooper et al. *Vet Path.* 2010. [2] Maffulli et al. *Br J Sports Med.* 2002. [3] Ong et al. *Lancet.* 2010. [4] Byers et al. *Am. J. Med. Genet.* 2017. Review. [5] Volk et al. *Cells Tissues Organs*. 2011. [6] Wang et al. *Matrix Biol.* 2020. [7] Miedel et al. *J Orthop Res.* 2015. [8] Beason et al. *J. Biomech*, 2012. [10] Dunkman et al. *Matrix Biol.* 2013. [11] Kjaer et al. *J. Anat.* 2006. [12] Miller KS, et al. *J Biomech Eng*. 2012. [13] Liu et al. *Proc Natl Acad Sci USA.* 1997.

ACKNOWLEDGEMENTS: *This study was supported by the Penn Center for Musculoskeletal Disorders (NIH/NIAMS AR069619) and NIGMS (R01GM124091).*

Determining Region-Specific Mechanical and Structural Differences in Aging Mouse Supraspinatus Tendons

Michael S. DiStefano[1], Biao Han[1], Patrick L. Paglia[1], Stephanie N. Weiss[1], Snehal S. Shetye[1], Andrew F. Kuntz[1], Louis J. Soslowsky[1]
[1]McKay Orthopaedic Research Laboratory, University of Pennsylvania, PA
micdis@seas.upenn.edu

Disclosures: AF Kuntz (5, Integra Lifesciences, Orthofix, Inc., FX Shoulder; 9, Orthopaedic Research Society, Phoenix Shoulder Society, American Shoulder and Elbow Surgeons, American Board of Orthopaedic Surgery), no other disclosures

INTRODUCTION: Damage, degeneration, and injury occur disproportionately in regions of high and complex stress, such as at the insertion site of the supraspinatus tendon of the shoulder, particularly in the aging population[1]. Recent studies in aged patellar tendons demonstrated an inferior response to load, reduced elastic and viscoelastic mechanical properties, and altered fibril structure[2]. However, despite its complex loading, region-specific mechanical and structural differences in aging mouse supraspinatus tendon remain unknown. Therefore, the objective of this study was to elucidate region-dependent mechanical and structural differences in mouse supraspinatus tendon with aging. We hypothesized that aging would result in region-specific mechanical and structural changes, such as inferior elastic and viscoelastic mechanical properties and altered collagen fibril morphology, with larger alterations expected at the insertion site due to the increased complexity and functional demands[3] in this region.

METHODS: Animals: Forelimbs were collected from male wildtype mice sacrificed at either 300 (P300, n=20) or 570 (P570, n=20) days of age, respectively (IACUC approved). Mechanics: Mice for mechanical testing were frozen at -20ºC until test day. Mice were thawed and the supraspinatus tendon-humerus complex from the left limb of each mouse was dissected clean. Stain lines were applied for optical strain tracking of the insertion and midsubstance regions and a laser device was used to measure cross-sectional area. The myotendinous junction was placed between two sandpaper tabs with cyanoacrylate. The humerus was secured in polymethyl methacrylate and the construct was mounted on a material testing machine (Instron 5848). Testing was conducted in a phosphate buffered saline bath at 37ºC. Each sample was preloaded to 0.025N. The testing protocol consisted of 10 cycles of preconditioning, followed by stress relaxations at 3%, 5%, and 7% strain. Following each stress relaxation, frequency sweeps of 10 cycles at 0.1, 1, 5, and 10 Hz were performed. Following a 10-minute rest, a quasistatic ramp-to-failure was completed. Viscoelastic parameters dynamic modulus (E*), phase shift (tan δ), and percent relaxation were quantified for each stress relaxation and frequency sweep. Elastic parameters stiffness and modulus were also calculated. Transmission Electron Microscopy (TEM): Supraspinatus tendons (n=4/age group) were isolated, fixed, and embedded in epon resin blocks. 85nm sections were cut using an ultramicrotome, stained with uranyless and phosphotungstic acid, and imaged at 60,000x using a transmission electronic microscope (JEOL 1010). Fibril diameter frequency distribution and fibril density were quantified. Statistics: Elastic properties were compared using two-way ANOVAs across age and region followed by Bonferroni post-hoc tests. Viscoelastic properties were compared using two-way ANOVAs across age and strain levels followed by Bonferroni post-hoc tests. Fibril diameter distributions were compared using Kolmogorov-Smirnov tests.

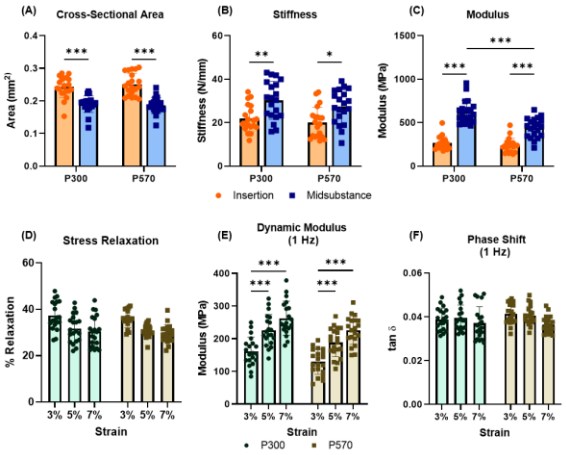

Figure 1. Elastic and viscoelastic mechanical properties. Insertion regions exhibited significantly greater (A) cross-sectional area while midsubstance regions had significantly greater (B) stiffness and (C) elastic modulus for both age groups. Elastic modulus was (C) significantly reduced with aging. Viscoelastic properties were conserved with aging with no differences across strain level in (D) stress relaxation and (F) phase shift and similar significant differences across strain levels in (E) dynamic modulus in both age groups. Data as mean ± standard deviation (*p≤0.05, **p≤0.01, ***p≤0.001)

RESULTS: Region-Dependent Elastic Mechanics (Fig. 1A-C): As expected, all samples failed at their insertion sites. Cross-sectional area was greater in the insertion region than in the midsubstance in both ages. Stiffness and modulus were lower for the insertion region than the midsubstance in the P300 and P570 groups. Midsubstance modulus had an interaction and decreased with age. Viscoelastic Mechanics (Fig. 1D-F): Although there were no interactions between viscoelastic properties and age, the viscoelastic response was preserved with aging across strain levels. Specifically, dynamic modulus was greater at 5 and 7% strain relative to 3% strain with aging. Additionally, percent relaxation and phase shift were not altered across strain levels with aging. Fibril Morphology (Fig. 2): Consistent with previous studies[4], fibril size distributions were different across region and age with smaller diameter fibrils at the insertion compared to the midsubstance within each age group. Moreover, insertion region fibrils had narrower distributions compared to the midsubstance fibrils whereas midsubstance fibrils demonstrated typical bimodal distributions for both age groups. Interestingly, aging resulted in a shift towards smaller diameter fibrils in the midsubstance region.

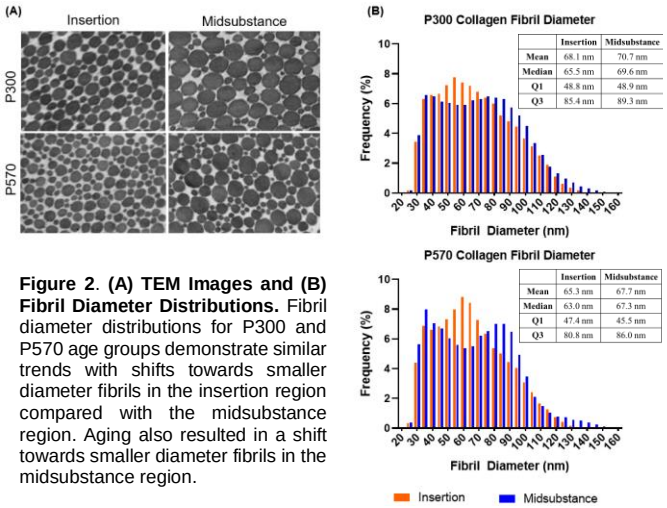

Figure 2. (A) TEM Images and (B) Fibril Diameter Distributions. Fibril diameter distributions for P300 and P570 age groups demonstrate similar trends with shifts towards smaller diameter fibrils in the insertion region compared with the midsubstance region. Aging also resulted in a shift towards smaller diameter fibrils in the midsubstance region.

DISCUSSION: This study investigated the regionally dependent mechanical and structural differences in aging mouse supraspinatus tendons. Supporting our hypothesis, detrimental mechanical and structural changes were observed at the insertion of supraspinatus tendons. Insertion region elastic mechanical properties were less than those at the midsubstance. Additionally, insertion region fibril size distributions shifted towards smaller fibril diameters. Previous studies in superficial digital flexor tendons demonstrated that mechanical properties and fibril diameter distributions can differ from the bone-tendon junction to the myotendinous junction[5]. Multiscale regression analyses have shown that the one of the strongest predictors of structure-function relationships at the insertion and midsubstance regions were mediators[6] of the relationship between fibril diameter and mechanical properties[6]. Contrary to our hypothesis, aging did not have a large influence on regional and whole tendon elastic and viscoelastic mechanical properties but did influence fibril morphology. Our results also agree with previous studies relating mechanical function to fibril morphology. Specifically, with increased loading, smaller diameter fibrils were not able to withstand the same loading and likely suffered early damage, resulting in inferior mechanical properties[3]. Our results support these previous findings and may further explain why supraspinatus tears predominantly occur at the tendon's insertion on the humeral head[7]. Future studies will build on these results by elucidating additional region-specific multiscale structural, functional, and compositional mechanisms in aging supraspinatus tendons.

SIGNIFICANCE: This study demonstrates critical region-specific mechanical and structural differences in aging mouse supraspinatus tendons.

ACKNOWLEDGEMENTS: *Study supported by NIH/NIAMS (AR070750) and Penn Center for Musculoskeletal Disorders (NIH/NIAMS, P30 AR069619).*

REFERENCES: 1. Buckwalter et al., J Bone Joint Surgery, 2003. 2. Dunkman et al., Matrix Biol, 2013. 3. Connizzo et al., Interface Focus, 2016. 4. Connizzo et al., J Orthop Res, 2016. 5. Watanabe et al., Connect Tissue Res, 2007. 6. Connizzo et al., J Biomech Eng, 2016. 7. Bell et al., J Orthop Res, 2015.

Collagen XII is a Critical Regulator of Tendon Function: Development of a Conditional Mouse Model

Ashley K. Fung[1,2], Mei Sun[3], Louis J. Soslowsky[1], David E. Birk[3]
[1]McKay Orthopaedic Research Laboratory, University of Pennsylvania, Philadelphia, PA
[2]Department of Bioengineering, University of Pennsylvania, Philadelphia, PA
[3]Department of Molecular Pharmacology and Physiology, University of South Florida, Tampa, FL
afung@seas.upenn.edu

Disclosures: Ashley K. Fung (N), Mei Sun (N), Louis J. Soslowsky (N), David E. Birk (N)

INTRODUCTION: Collagen XII is a fibril-associated collagen with interrupted triple helices (FACIT) that regulates collagen fibril assembly, and mutations in *Col12a1* result in myopathic Ehlers-Danlos Syndrome (mEDS). Patients with mEDS experience excess weakness at birth, hypermobile distal joints, and an absence of deep tendon reflexes [1], indicating impaired tendon function due to the absence of collagen XII. Tendons in a global *Col12a1*$^{-/-}$ knockout mouse model demonstrated disrupted grip strength and tendon fiber structure as well as disordered tenocyte organization [2]. However, secondary effects due to involvement of bone and muscle may occur in this model, and the isolated role of collagen XII in tendon has not been elucidated. To address this limitation, the objective of this study was to create and characterize a conditional *Col12a1*-null mouse model to target collagen XII knockout in tendons using a Scleraxis-Cre driver. We hypothesized that tendon-targeted knockout of *Col12a1* expression would impair tendon function.

METHODS: Model Development: A promoter-driven knockout embryonic stem (ES) cell line was obtained from the KOMP Repository (ID: CSD29388, *Col12a1*$^{tm2a(KOMP)Wtsi}$). ES cell clones were injected into wild-type C57BL/6-Albino blastocysts, and resulting chimeric mice were backcrossed to produce mice with the targeted allele, *Col12a1*$^{+/ta}$. *Col12a1*$^{+/ta}$ mice were bred with FLPe mice (B6; SJL-Tg(ACTFLPe) 9205Dym/J, Jackson Labs) to excise the FRT flanked neo sequences. The resulting offspring were crossbred with C57BL/6 mice for 6 generations and then inter-crossed to obtain conditional knockout mice, *Col12a1*$^{flox/flox}$. *Col12a1*$^{flox/flox}$ mice were bred with Scleraxis-Cre (*Scx-Cre*) mice to obtain tendon-targeted heterozygous (Het, *Col12a1*$^{+/\Delta ten}$) and homozygous (KO, *Col12a1*$^{\Delta ten/\Delta ten}$) collagen XII knockout mice. Gene & Protein Expression: *Col12a1* expression and collagen XII content were assessed in flexor digitorum longus (FDL) tendons from mice at day 10 using qPCR and Western blots, respectively. Immunofluorescence: FDLs were dissected, fixed in 4% paraformaldehyde, embedded in optimal cutting temperature compound, and sectioned in the transverse plane at 5 μm thickness. Immunofluorescence staining of collagen XII was performed using a rabbit anti-mouse Col XII antibody (KR33, 1:500 dilution) with a donkey anti-rabbit Alexa Fluor 568 (1:200 dilution) secondary antibody. Grip Strength: Using a grip strength meter, mice were lowered toward the grip platform and upon grasping, mice were pulled away steadily until the grip was broken. The force applied just before the mouse lost its grip was recorded as the peak force. Tendon Mechanics: FDL tendons from day 60 mice were dissected from the foot, cleaned of excess tissue, and mechanically evaluated as described [3]. Tensile testing was performed using the following protocol: preconditioning, stress relaxation at 5% strain, and a ramp to failure at a rate of 0.5%/s. Statistics: One-way ANOVAs with Tukey post-hoc tests were conducted. Significance was set at $p \leq 0.05$.

RESULTS: *Col12a1* expression was reduced in *Col12a1*$^{\Delta ten/\Delta ten}$ KO mice compared to Cre- littermate control (Ctrl) mice though baseline expression, determined from traditional collagen XII knockout mice [2], was not reached in KO mice (**Fig. 1A**). Furthermore, the α1(XII) chain was present at comparable levels in the control group: Cre-, *Scx-Cre* and *Col12a1*$^{flox/flox}$ mice (data not shown). Collagen XII content was lower in Het mice and just above background in KO mice compared to Ctrl (**Fig. 1B**). Collagen XII immunofluorescence localization demonstrated efficient knockdown in the tendon proper but not in the surrounding peritenon as expected (**Fig. 1C**). For joint function, female KO mice had reduced forelimb grip strength compared to Het (**Fig. 2A**) while male KO mice had reduced strength compared to Ctrl mice (**Fig. 2B**). At the tendon level, FDLs from day 60 male and female KO mice exhibited a reduction in mechanical properties. There was no difference in cross-sectional area (data not shown), but stiffness and modulus were both decreased in KO FDLs compared to Ctrl (**Fig. 2C, D**).

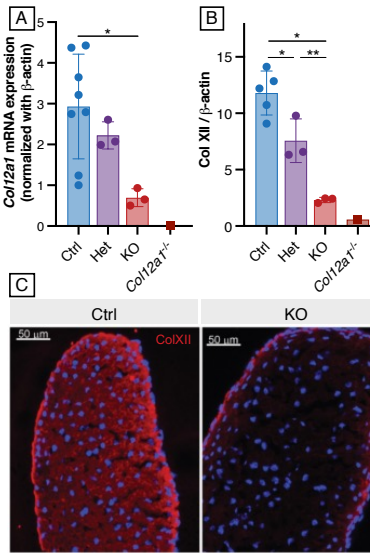

Figure 1: A) *Col12a1* and B) collagen XII expression were significantly reduced in *Col12a1*$^{\Delta ten/\Delta ten}$ KO tendons compared to Ctrl though still above the baseline level established from conventional *Col12a1*$^{-/-}$ mice. C) Efficient collagen XII knockdown was achieved in the tendon proper of KO tendons but not the surrounding peritenon. (*p≤0.05, **p≤0.01)

DISCUSSION: The overall goal of this study was to create a conditional *Col12a1*-null mouse model and target collagen XII knockout to tendons using a scleraxis-Cre driver. In FDLs of tendon-targeted *Col12a1*$^{\Delta ten/\Delta ten}$ KO mice, both mRNA and protein expression levels were decreased but did not reach the baseline levels of global collagen XII knockout mice. This suggests that cells from a non-tendon lineage are not targeted as expected, and collagen XII immunofluorescence indicates that the surrounding peritenon population likely contributes to the above baseline expression levels. Furthermore, in the absence of *Col12a1* expression and therefore collagen XII, *Col12a1*$^{\Delta ten/\Delta ten}$ KO mice have impaired mechanics, as evidenced by reduced forelimb grip strength and FDL tendon mechanical properties. Reduced grip strength is consistent with joint function in the global *Col12a1*$^{-/-}$ knockout model, but interestingly, FDL tendon mechanical properties deviated from previous findings. In the global *Col12a1*$^{-/-}$ knockout model, FDLs had larger cross-sectional area and greater stiffness with no difference in tendon material properties [2]. In this study, however, there were no differences in FDL cross-sectional area in KO mice, but stiffness was significantly decreased, resulting in inferior tendon elastic modulus. Differences in mechanical properties suggest that collagen XII is a critical regulator of tendon structure-function, and the contrasting findings from the global knockout model may be a result of secondary effects, such as those due to muscle and bone. Additionally, collagen XII knockout did not exhibit sex-specific effects with similar trends in grip strength and tendon mechanics for both male and female mice. Future studies are necessary to elucidate sex-specific roles of collagen XII in tendon structure and determine the biological mechanisms underlying changes in tendon structure-function. In conclusion, grip strength and tendon mechanical changes in the tendon-targeted *Col12a1*$^{\Delta ten/\Delta ten}$ model support that collagen XII is a critical regulator of tendon function.

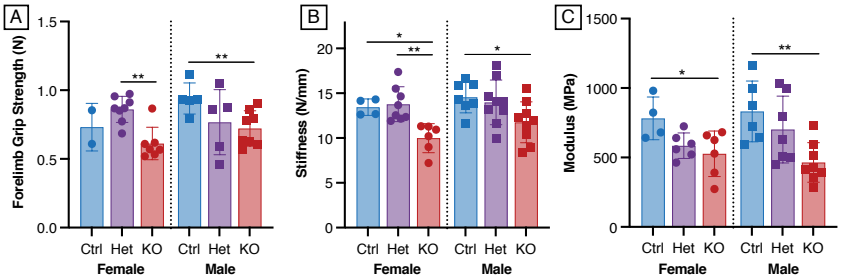

Figure 2: Forelimb grip strength was significantly reduced in A) female *Col12a1*$^{\Delta ten/\Delta ten}$ KO mice compared to *Col12a1*$^{\Delta ten/+}$ Het and in male *Col12a1*$^{\Delta ten/\Delta ten}$ KO mice compared to Ctrl. FDL tendon B) stiffness and C) modulus were significantly reduced in *Col12a1*$^{\Delta ten/\Delta ten}$ KO compared to Ctrl in both female and male mice. (*p≤0.05, **p≤0.01)

SIGNIFICANCE: Through development of a tendon-targeted collagen XII knockout mouse model, this study demonstrates the critical role of collagen XII in regulating joint and tendon function. Elucidating guiding mechanisms will provide the foundation to leverage the role of collagen XII in therapeutic strategies, providing support for treatments that address conditions such as myopathic Ehlers-Danlos syndrome.

REFERENCES: [1] Zou et al., Hum Mol Genet, 2014 [2] Izu et al., Matrix Biology, 2021 [3] Sun et al., Matrix Biology, 2020.

ACKNOWLEDGEMENTS: This study was funded by NIH/NIAMS (R01AR078790) and the Penn Center for Musculoskeletal Disorders (P30AR069619).

Knockdown of Decorin and Biglycan at Time of Tendon Injury Alters Gene Expression and Fibril Morphology

Ashley K. Fung[1,2], Thomas P. Leahy[1,2], Stephanie N. Weiss[1], Sheila M. Adams[3], Nathaniel A. Dyment[1], David E. Birk[3], Louis J. Soslowsky[1]
[1]McKay Orthopaedic Research Laboratory, University of Pennsylvania, Philadelphia, PA, [2]Department of Bioengineering, University of Pennsylvania
[3]Department of Molecular Pharmacology and Physiology, University of South Florida, Tampa, FL
afung@seas.upenn.edu

Disclosures: All authors have nothing to disclose.

INTRODUCTION: Tendon healing follows a typical wound healing process, including inflammatory, proliferative, and remodeling phases, though outcomes following tendon injury remain poor. The small leucine-rich proteoglycans (SLRPs), decorin (Dcn) and biglycan (Bgn), are critical regulators of fibrillogenesis and matrix assembly, but their specific roles in tendon healing are not fully understood. We previously showed that knockdown of Bgn or both Dcn/Bgn resulted in increased tendon modulus 6-weeks post-injury, suggesting improved function due to Bgn knockdown [1]. However, the mechanisms driving these differences remain unknown. Therefore, the objective of this study was to define the biological and structural regulatory roles of Dcn and Bgn in tendon healing using conditional knockdown of Dcn, Bgn, and both Dcn/Bgn at the time of injury. We hypothesized that induced knockdown of Bgn and both Dcn/Bgn would improve healing resulting in increased tendon extracellular matrix gene expression, reduced scarring, and superior fibril structure compared to wild-type mice.

METHODS: Study design: Female $Dcn^{+/+}/Bgn^{+/+}$ control (WT, n=44), $Dcn^{flox/flox}$ (I-$Dcn^{-/-}$, n=32), $Bgn^{flox/flox}$ (I-$Bgn^{-/-}$, n=32), and compound $Dcn^{flox/flox}/Bgn^{flox/flox}$ (I-$Dcn^{-/-}/Bgn^{-/-}$, n=32) mice with a tamoxifen inducible Cre (B6.129-Gt(ROSA)26Sortm1(cre/ERT2)Tyj/J, Jackson Labs) were used [2] (IACUC approved). At 120 days old, Cre excision was induced via two (injured) or three (uninjured) consecutive daily IP injections of tamoxifen. At time of induction, injured groups underwent bilateral patellar tendon (PT) injury surgery as described [3] and were sacrificed 1-, 3- or 6-weeks later. Uninjured groups were sacrificed at 150 days old. Gene Expression: PTs (n=4/group) were homogenized, and RNA was extracted. RNA was converted to cDNA, pre-amplified, and loaded into a Fluidigm 96.96 Dynamic Array. The 96 target genes included categories of collagens, non-collagenous matrix, matrix remodeling, cell-ECM proteins, and cell and inflammatory markers. ΔCt was calculated by subtracting the gene cycle threshold (Ct) from average Ct of the housekeeping genes (*Abl1*, *Rps17*). Histology: Knee joints (n=4/group) were fixed, decalcified, and paraffin sectioned in the transverse plane of the PT at 10μm. Sections were stained with toluidine blue, and scar tissue was measured in the wound site adjacent to the native tissue. Transmission Electron Microscopy: PTs (n=4/group) were isolated, fixed, and processed as described [4]. Sections were cut at 85nm, stained, and imaged at 60,000x in the wound area. Fibril diameter distributions were quantified. Statistics: For gene expression and scar area percentage, one-way ANOVAs with Tukey post-hoc tests were conducted at each timepoint. Fibril diameter distributions were compared using Kolmogorov-Smirnov tests. Significance was set at $p \leq 0.05$ and trends at $p \leq 0.1$.

RESULTS: Gene Expression**:** *Dcn* and *Bgn* expression demonstrated efficient knockdown at each healing timepoint. *Dcn* was significantly reduced (4-6 fold) in I-$Dcn^{-/-}$ and I-$Dcn^{-/-}/Bgn^{-/-}$ tendons compared to WT and I-$Bgn^{-/-}$ mice (**Fig 1A**). Similarly, *Bgn* expression was 4-6 fold lower in I-$Bgn^{-/-}$ and I-$Dcn^{-/-}/Bgn^{-/-}$ tendons (**Fig 1B**). Further evaluation of gene expression profiles revealed subtle changes during early tendon healing. At 1-wk post-injury, *Col12a1*, *Tnmd*, and *Igf1* (**Fig 2A**) expression were significantly reduced in I-$Dcn^{-/-}$ tendons compared to WT. By 3-wks, *Igf1* expression in the I-$Dcn^{-/-}$ group was significantly greater than WT tendons, contrasting the difference at 1-week. And by 6-wks, there was no difference in *Igf1* expression between WT and I-$Dcn^{-/-}$ tendons, while expression was significantly higher in the I-$Dcn^{-/-}/Bgn^{-/-}$ group compared to WT tendons (**Fig 2A**). Contrasting the subtle changes at 1- and 3-wks post-injury, several significant gene changes during late tendon healing at 6-wks were observed in I-$Dcn^{-/-}/Bgn^{-/-}$ tendons. For example, there were no differences in *Fmod* at 1 or 3 wks, but *Fmod* was significantly increased at 6 wks compared to WT (**Fig 2B**). Similar trends were observed across several target genes, and those exhibiting increased expression in the I-$Dcn^{-/-}/Bgn^{-/-}$ group compared to WT at 6-weeks are listed in **Fig 2C**. Histology & Fibril Morphology: No differences in scar area percentage were observed at any healing timepoint (data not shown). However, fibril size distributions were significantly different between all groups at each timepoint with a shift towards smaller diameter fibrils in the I-$Dcn^{-/-}/Bgn^{-/-}$ at both 3- and 6-wks post-injury compared to WT and I-$Dcn^{-/-}$ (**Fig 3A,B**). Additionally, the fibril diameter distribution was narrower in I-$Bgn^{-/-}$ tendons compared to WT and I-$Dcn^{-/-}$ at 6-wks (**Fig 3B**).

DISCUSSION: Using our novel inducible models to minimize compensation typically present in traditional models, our findings support biological and structural regulatory roles of Dcn and Bgn during tendon healing, as evidenced by alterations in gene expression profiles and fibril structure. In addition to their structural roles in fibrillogenesis and matrix assembly, Dcn and Bgn regulate inflammation and growth factor activity [5]. Though only moderate changes were observed in 1- and 3-weeks post-injury, increased expression of several growth factors and matrix proteins at 6-weeks post-injury suggest that Dcn and Bgn play more critical roles during the remodeling phase of healing. This may be due to the role of Dcn and Bgn in regulating signaling pathways such as Igf, Pdgf, and Tgfb, which results in downstream effects on matrix synthesis and remodeling [6]. While no compensatory changes in *Dcn* or *Bgn* expression were observed, the most pronounced effects in the I-$Dcn^{-/-}/Bgn^{-/-}$ group indicate overlapping functions of Dcn and Bgn and that functional compensation may occur in the single knockdown models [7,8]. Contrary to our hypothesis, induced knockdown of Bgn in both the single and double knockdown groups resulted in a narrower distribution of fibril diameters at 6-weeks post-injury, which deviates from an uninjured distribution. Therefore, increased modulus in the I-$Bgn^{-/-}$ and I-$Dcn^{-/-}/Bgn^{-/-}$ groups is likely not due to superior fibril structure and may instead be driven by alterations in the non-collagenous matrix [1]. Future work is necessary to elucidate the roles of decorin and biglycan in regulating growth factor activity and evaluate the composition of the healing matrix.

SIGNIFICANCE: This study revealed regulatory roles of decorin and biglycan in altering gene expression and fibril structure during tendon healing, and elucidating these roles are necessary for understanding mechanisms that drive poor tendon healing.

REFERENCES: [1] Fung et al., ORS Annual Meeting, 2020. [2] Robinson et al., Matrix Biology, 2017. [3] Lin et al., J Biomech, 2006. [4] Dunkman et al., Matrix Biology, 2014 [5] Iozzo et al., J Biol Chem, 2011 [6] Hildebrand et al., Biochem J, 1994, [7] Corsi et al., JBMR 2002, [8] Wadhwa et al., Bone 2007

ACKNOWLEDGEMENTS: We thank Jaclyn Carlson, Michael DiStefano, and Ryan Leiphart for their assistance. This study was funded by NIH/NIAMS (R01AR068057) and the Penn Center for Musculoskeletal Disorders (P30AR069619).

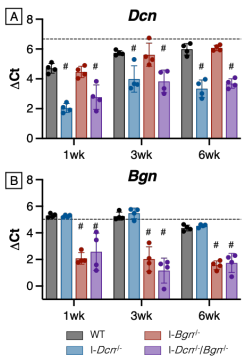

Fig 1: Induced knockdown of A) *Dcn* and B) *Bgn* expression resulted in a significant reduction in expression levels. (#: p≤0.05 from WT). Uninjured WT expression level is shown as a dashed line.

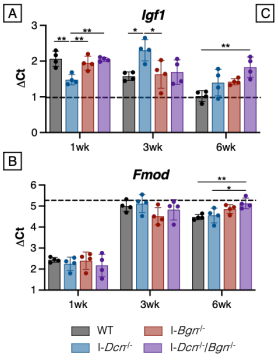

C

Gene	ΔCt diff	p-value
Collagens		
Col1a2	0.67	0.006
Col6a1	0.55	0.008
Col11a1	0.58	0.02
Non-Collagenous Matrix		
Fbn2	1.97	0.005
Fmod	0.65	0.01
Hspg2	0.49	0.01
Thbs4	0.83	0.009
Tnc	0.48	0.05
Matrix Remodeling		
Adamts2	0.42	0.006
Mmp2	0.73	0.007
Mmp3	1.38	0.001
Mmp14	0.96	0.003
Cell-ECM		
Itga11	0.65	0.01
Ptk2	0.36	0.005

Gene	ΔCt diff	p-value
Signaling		
Bmp2	0.5	0.02
Igf1	0.81	0.003
Mtor	0.47	0.001
Pdgfa	0.55	0.009
Pdgfb	0.59	0.009
Pdgfrb	0.47	0.04
Tgfb1	0.51	0.006
Tgfb3	0.66	0.005
Vegfb	0.57	0.01
Cell Cycle/Proliferation		
Cdkn1a	0.61	0.02
H2afx	0.49	0.02
Inflammation		
Ccl4	1.61	0.02
Pge2	0.33	0.05

Fig 2: A) I-$Dcn^{-/-}$ tendons exhibited an altered healing profile of *Igf1* expression with a significant decrease at 1-week and increase at 3-weeks post-injury compared to WT tendons. At 6-weeks post-injury *Igf1* and B) *Fmod* expression were significantly increased in I-$Dcn^{-/-}/Bgn^{-/-}$ tendons compared to WT tendons. Uninjured WT expression level is shown as a dashed line. (*p≤0.05, **p≤0.01) C) Target genes exhibiting increased expression in I-$Dcn^{-/-}/Bgn^{-/-}$ tendons compared to WT tendons at 6-weeks post-injury. The signaling category had the greatest number of differentially expressed genes. ΔCt diff represents the increase in mean ΔCt of I-$Dcn^{-/-}/Bgn^{-/-}$ compared to WT.

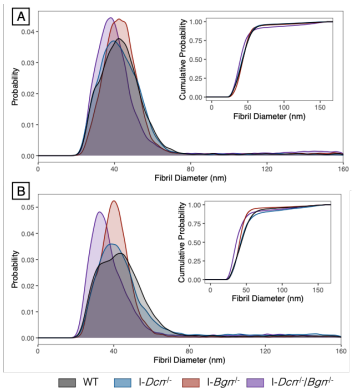

Fig 3: Probability density and cumulative distribution (inset) plots of fibril diameter demonstrated a moderate shift towards smaller fibril diameters in the I-$Dcn^{-/-}/Bgn^{-/-}$ group at A) 3-weeks and B) 6-weeks post-injury. I-$Bgn^{-/-}$ tendons also had a narrower distribution of fibril diameters at 6-weeks compared to I-$Dcn^{-/-}$ and WT tendons.

Region and Strain-Dependent Mechanics of Supraspinatus Tendons are Influenced by Fibril Modulus and Sliding

Biao Han, Michael DiStefano, Snehal S. Shetye, Andrew F. Kuntz, Louis J. Soslowsky
McKay Orthopaedic Research Laboratory, University of Pennsylvania, Philadelphia, PA

Disclosures: AF Kuntz (5, Integra Lifesciences, Orthofix, Inc., FX Shoulder; 9, Orthopaedic Research Society, Phoenix Shoulder Society, American Shoulder and Elbow Surgeons, American Board of Orthopaedic Surgery), no other disclosures

INTRODUCTION: Rotator cuff impairments are a common disorder [1], significantly impacting quality of life, leading to pain, disability, and decreased independence. With aging, tendon exhibits altered fibril structure and inferior mechanical properties [2,3,4], with differential fibril behavior in the midsubstance compared to the insertion region [5]. However, the relationship between macroscopic tendon and microscopic fibril mechanical behavior remains poorly understood. Therefore, the objective of this study was to determine the macroscopic and microscopic tensile mechanical properties of rotator cuff tendon (supraspinatus). We hypothesized that the response of tendon to tensile load is region and strain dependent, and informed by the deformation, sliding and modulus of individual fibrils.

METHODS: *Sample Preparation and Mechanical Tests*. Male wild-type (WT) mice ($n \geq 9$ for each group, 30 mice total) were sacrificed at P150 (IACUC approved). The supraspinatus tendon-bone complex was dissected and prepared as described [6,7]. For macroscopic mechanical tests, tendons underwent 10 cycles of preconditioning, followed by stress relaxation at 3%, 5%, and 7% strain, and then ramp-to-failure. Following each stress relaxation, frequency sweeps of 10 cycles at 0.1, 1, 5, and 10 Hz were performed. For the microscopic fibril behavior study, tendons underwent 10 cycles of preconditioning, followed by a 1-minute hold at 0 N and then stretch to a randomly assigned grip-to-grip strain level (1, 5 or 9%, consistent with the toe, early linear and late linear regions, respectively [3]) at 0.1% strain per second. Then, the tendon was flash frozen, cryo-sectioned, and fixed. *Macroscopic Location-Dependent Mechanical Properties.* Cross-sectional area was measured using a laser device [8]. Strains in the insertion and midsubstance regions were measured optically. Quasistatic mechanical parameters including stiffness and modulus were calculated from the ramp-to-failure data. *Macroscopic Strain Dependent Mechanical Properties.* Viscoelastic parameters dynamic modulus (E^*), tangent of phase shift ($\tan(\delta)$) and percent relaxation were quantified for each stress relaxation and corresponding frequency sweeps. *Microscopic Fibril Behavior and Mechanical Properties.* AFM nanomechanical mapping of 2μm × 2μm regions was performed with the PeakForce QNM mode on a Bioscope Catalyst AFM following a modified protocol [5]. Fibril D-period and indentation modulus were analyzed for ~20 fibrils from each image across multiple sections using a custom program. An increase in the fibril D-period is considered as fibril stretch, while a change in variance is indicative of fibril sliding [5]. *Statistical Analyses*. Mann-Whitney U-tests were performed on cross-sectional area, stiffness, modulus and percent relaxation data. Two-way mixed model ANOVA tests were performed on E^*, $\tan(\delta)$ and D-period data, with location and strain as the independent variables. Comparison of variance was performed using a Bartlett's test with post-hoc F-test. Significance was set at $p < 0.05$.

RESULTS: *Macroscopic Location Dependent Mechanical Properties.* Despite no differences in cross-sectional area (Fig. 1a), the insertion and midsubstance of the supraspinatus tendon exhibited differences in stiffness and modulus (Fig. 1b). *Macroscopic Strain Dependent Mechanical Properties.* Increasing strain from 3%, to 5% and then to 7% led to an increase in the dynamic modulus under all frequencies (Fig. 2a) and a decrease in percent relaxation (Fig. 2b). *Microscopic Fibril Behavior and Mechanical Properties.* Increasing strain from 1% to 5% and from 5% to 9% resulted in no difference in fibril stretch (Fig. 3a), while fibril sliding was increased between 5% and 9% (Fig. 3b). Fibril deformation and sliding were not different between insertion and midsubstance (Fig. 3a and b). However, fibril modulus was decreased at the insertion compared to midsubstance (Fig. 3c).

DISCUSSION: We measured the macroscopic tensile mechanical properties and the microscopic collagen fibril deformation, sliding and indentation modulus of the insertion and midsubstance of the murine supraspinatus tendon. We found that the supraspinatus tendon exhibits substantial regional diversity in mechanics, structure, and composition at both the macro- and microscopic scales. Consistent with previous findings [5,6], the strain dependence of the supraspinatus tendon was not associated with microscopic collagen fibril stretch, while we did observe changes in viscoelastic mechanics and collagen fibril sliding in the linear region of the stress-strain curve, supporting the concept that inter-and intra-fibril mechanisms contribute to the overall mechanical response. Conversely, the absence of fibril deformation and sliding in the toe and early linear regions is likely caused by fibrils uncrimping and re-alignment [3,9]. In addition to previous findings of strain- and region-dependent fibril stretch and sliding [5], we found that macroscopic region-dependent mechanics are associated with fibril indentation modulus. We therefore speculate that due to different and complex loading environments, the insertion region of the supraspinatus tendon developed weaker fibrils compared to the midsubstance during maturation, which contributes to the likelihood of lesions at the insertion [10]. Further studies should address the cause of these interesting findings and could include measurement of region-dependent fibril diameter distributions [11] and cross-linking within fibrils [12].

SIGNIFICANCE: This study extends our understanding of the relationship between the macroscopic and microscopic mechanical properties of tendons.

ACKNOWLEDGEMENT: This study was supported by NIH/NIAMS (AR070750) and the Penn Center for Musculoskeletal Disorders (NIH/NIAMS, P30 AR069619).

REFERENCES: [1] Buckwalter JA et al. *JBJS* 2003, 85, 748-58. [2] Buckley MR et al. *J Biomech Eng* 2013, 135, 041005. [3] Connizzo BK et al. *J Biomech Eng* 2013, 135, 021019. [4] Dunkman AA et al. *Matrix Biol* 2013, 32, 3-13. [5] Connizzo BK et al. *J Biomech* 2014, 47, 3794-8. [6] Connizzo BK et al. *J Orthop Res* 2015, 33, 882-8. [7] Connizzo BK et al. *Interface Focus* 2016, 6, 20150043. [8] Favata M University of Pennsylvania, 2006. [9] Miller KS et al. *J Biomech* 2012, 45, 2061-5. [10] Littlewood C et al. *J Man Manip Ther* 2012, 20, 209-13. [11] Ansorge HL et al. *Ann Biomed Eng* 2011, 39, 1904-13. [12] Marturano J et al. *Acta biomater* 2014, 10, 1370-9.

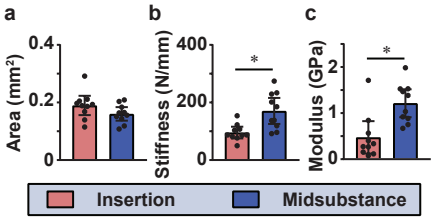

Fig. 1 Insertion and midsubstance regions of supraspinatus tendons exhibit **a)** no difference in cross sectional area. Insertion region was decreased compared to midsubstance for **b)** stiffness and **c)** modulus.
*: $p < 0.05$.

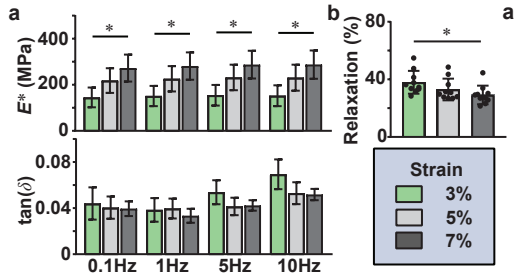

Fig. 2 Supraspinatus tendons show strain dependent behaviors. **a)** Increased dynamic modulus from 3% to 7% strain, with no difference in tan(δ) and **b)** Decreased percent relaxation from 3% to 7% strain. *: $p < 0.05$.

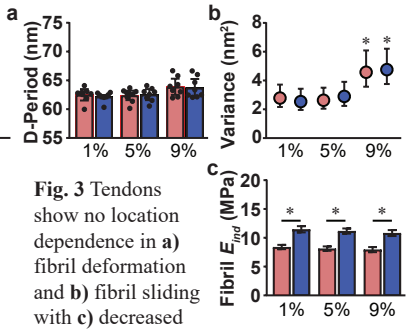

Fig. 3 Tendons show no location dependence in **a)** fibril deformation and **b)** fibril sliding with **c)** decreased insertion fibril modulus compared to midsubstance. *: $p < 0.05$.

FAK Inhibition Attenuates Increased Tendon Cell Nuclear Aspect Ratio with Applied Mechanical Strain In Situ

Thomas P. Leahy[1], Nathaniel A. Dyment[1], Louis J. Soslowsky[1]
[1]McKay Orthopaedic Research Laboratory, University of Pennsylvania, PA
tpleahy@seas.upenn.edu.

Disclosures: Thomas P. Leahy (N), Nathaniel A. Dyment (N), Louis J. Soslowsky (N)

INTRODUCTION: Tendons carry tensile loads via their dense extracellular matrix (ECM), which transmits mechanical strain to the resident cells. Regulatory mechanical cues maintain tendon homeostasis, as unloading and overloading both result in reduced ECM organization and mechanical integrity as well as loss of tendon cell phenotype, including changes in cell and nuclear shape and reduced tenogenic gene expression.[1–3] Focal adhesion kinase (FAK) is an intracellular protein kinase that plays a critical role in regulating cell-ECM attachment as well as turnover of the mechanosensitive actin network that transmits mechanical cues from the plasma membrane to the nucleus. While FAK activation is required for tenogenic gene expression in response to stimulation by growth factors and mechanical stretching,[4–6] the mechanism by which FAK activity regulates the cell's ability to sense mechanical stretching within the *in situ* tendon environment is unknown. Therefore, the objective of this study was to evaluate the effects of FAK inhibition on tendon cell nuclear response to mechanical strain within the *in situ* tendon ECM. We hypothesized that increases in nuclear aspect ratio (nAR) in response to applied macroscale strain would be attenuated in tendons treated with a FAK inhibitor compared to untreated tendons.

METHODS: Study Design: Flexor digitorum longus (FDL) tendons from male WT adult mice were freshly dissected and maintained in DMEM supplemented with 5% FBS and 25 mM HEPES. Tendons were randomized to untreated and FAK-inhibited (FAK-I) groups (n=5-6 tendons per group). For FAK-I tendons, media was supplemented with 10 µM PF-573228 (Tocris; Minneapolis, MN) for 1 hour at 37C, while the untreated tendons were maintained for 1 hour at 37C. Following treatment, cell nuclei were stained with DRAQ5 (1:1000) for 30 minutes, mounted within a custom mechanical loading device, and imaged with confocal microscopy at 0, 5, and 10% applied strain (Fig 1A-B). Nuclei were segmented with FIJI, nAR computed, and manually tracked between strain levels (n=12-36 nuclei per tendon).[7] Live/dead staining was performed with calcein-AM and ethidium homodimer-1 (ThermoFisher; Waltham, MA) to confirm tissue viability within the loading system. Mechanical Loading Device: We developed a custom mechanical loading device to apply strain to a tendon sample while being imaged on an inverted confocal microscope. The device consists of 2 linear actuators that apply mechanical strain to the tendon, along with a 20 lb. (88.96 N) load cell to monitor load. Manual stages center the tendon in the x and z directions over the objective and place it within the objective working distance. Custom LabView software was developed to operate the device, including centering the tendon over the objective in the y direction and applying mechanical strain based on the gauge length. Confocal Imaging: Confocal imaging was performed with a Zeiss LSM 710 confocal microscope while the tendon was mounted and maintained at the desired strain level. Imaging was performed with a 633nm excitation laser and 10x objective by imaging through the maximum light penetration depth at a z-stack interval of 5 µm.

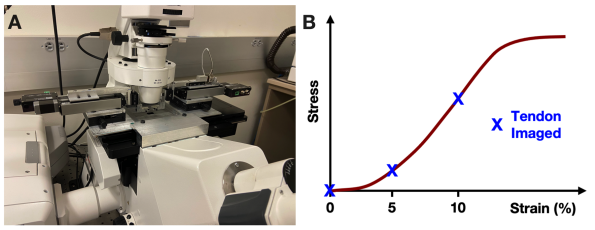

Figure 1. Custom Mechanical Loading Device. A) Fabricated device mounted on a Zeiss LSM 710 inverted confocal microscope. B) Stress-strain curve indicating image capture locations at 0, 5, and 10% strain.

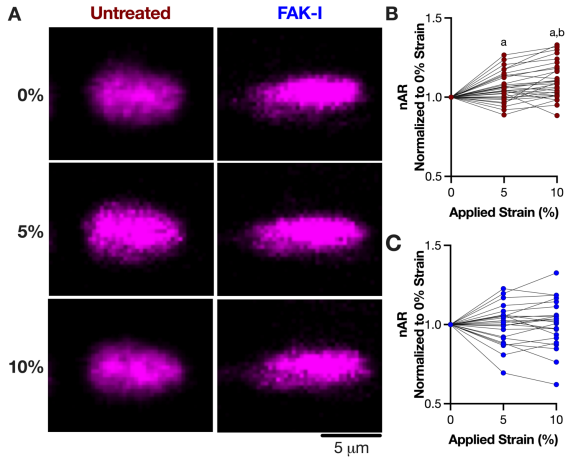

Figure 2. Increases in nAR with increasing applied strain are attenuated by FAK inhibition. A) Representative images for untreated and FAK-I nuclei at the indicated applied strain value. nAR plotted across strain values for B) untreated and C) FAK-I samples. Statistical comparison performed on non-normalized data (data not shown) between strain levels using repeated measures one-way ANOVA with Tukey's post-hoc tests (significance at $p \leq 0.05$). a, significant increase relative to 0% strain; b, significant increase relative to 5% strain.

RESULTS: Live/dead staining indicated that the tissue was viable with no differences between untreated and FAK-I tendons (data not shown). Nuclei tracked across strain levels in untreated tendons became increasingly elongated with applied strain (Fig 2A-B), while the nuclei from FAK-I treated tendons did not elongate across strain levels (Fig 2A,C). Across tendons, normalized nAR was decreased at both 5% and 10% strain in FAK-I tendons relative to untreated tendons (Fig 3).

DISCUSSION: Consistent with our hypothesis, FAK-I treatment attenuated the increases in nAR with applied strain observed in the untreated tendons both within tendons (Fig 2) and across all tendons measured (Fig 3). These results indicate that FAK regulates ECM to nucleus strain transmission in tendon cells. Previous studies demonstrated that intact actin networks are required for maintenance of tendon cell fate, collagen fibril deposition, collagen crosslinking, and re-tensioning the ECM.[8–10] Given FAK's role in establishing focal adhesions to tether actin networks to the ECM, it is not surprising that FAK is required for tenogenic gene expression.[4–6] Results from the present study suggest that the dependence on FAK for tenogenic gene expression may due to its role in regulating nuclear mechanosensitivity. The rapid effect of FAK inhibition on nuclear response to strain suggests that tendon cells regularly turn over their actin networks and reestablish focal adhesions to actively probe their local mechanical environment. This result is particularly interesting in mature tendon cells encased in established ECMs, where the local mechanical environment is presumably stable.

SIGNIFICANCE: This study evaluated the effects of FAK inhibition on nuclear response to mechanical strain within *in situ* tendon ECM. We found that inhibition of FAK attenuated increases in nAR with applied strain, which suggests that FAK is required for tendon cell sensation of its surrounding mechanical environment.

ACKNOWLEDGEMENTS: We acknowledge financial support from NIH/NIAMS (T32AR007132 and P30AR069619). We also acknowledge support from Andrea Stout and the PSOM Cell and Developmental Biology Microscopy Core.

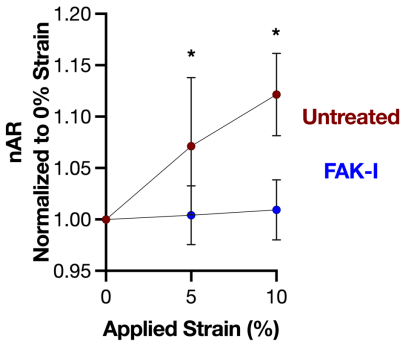

Figure 3. Increases in nAR with increasing applied strain were consistently attenuated by FAK inhibition across all samples. Data is represented as mean normalized nAR ± standard deviation for each group. Statistical comparison performed using t-tests to compare treatment groups at 5% and 10% strain (significance at $p \leq 0.05$). *, significant difference between groups at strain value.

REFERENCES: 1. Wunderli *et al.*, JOR, 2018; 2. Yamamoto *et al.*, J Biomech Eng, 2002; 3. Soslowsky *et al.*, JSES, 2000. 4. Liu *et al.*, Stem Cells Int, 2018; 5. Xu *et al.*, J Cell Physiol, 2012; 7. Schindelin *et al.*, Nat Methods, 2012; 8. Gardner *et al.*, JOR, 2012; 9. Canty *et al.*, J Biol Chem, 2006; 10. Schiele *et al.*, JOR, 2015.

Knockdown of Decorin and Biglycan During the Early Proliferative and Remodeling Phases of Tendon Healing Alters Gene Expression and Fibril Morphology

Thomas P. Leahy[1], Ashley K. Fung[1], Stephanie N. Weiss[1], Sheila M. Adams[2], Nathaniel A. Dyment[1], David E. Birk[2], Louis J. Soslowsky[1]
[1]McKay Orthopaedic Research Laboratory, University of Pennsylvania, PA
[2]Department of Molecular Pharmacology and Physiology, University of South Florida, Tampa, FL
tpleahy@seas.upenn.edu

Disclosures: All authors have nothing to disclose.

INTRODUCTION: Tendon matrix consists of highly organized collagen fibrils with small leucine rich proteoglycans (SLRPs) bound to the fibril surface. The SLRPs decorin (gene: *Dcn*) and biglycan (gene: *Bgn*) play a critical role in regulating fibrillogenesis during tendon development and following tendon injury.[1-3] Previous studies have demonstrated that *Bgn* knockdown alone or in tandem with *Dcn* knockdown during healing resulted in improved tendon mechanical properties, regardless of knockdown induction timepoint.[4-5] Surprisingly, *Dcn* knockdown alone had no measurable effect on healing tendon mechanical properties. While these prior studies demonstrated that knockdown of SLRPs could improve tendon mechanical properties, they did not define the mechanism by which SLRP knockdown altered the biological processes and matrix structure within the healing tendon. Therefore, the objective of this study was to define the roles of decorin and biglycan in modulating tendon morphology, gene expression, and collagen ultrastructure throughout the phases of tendon healing. We hypothesized that *Bgn* knockdown alone or in tandem with *Dcn* knockdown would lead to faster recovery of healthy tendon properties, including increased tendon-specific extracellular matrix gene expression, reduced scarred matrix, and a return to an uninjured distribution of collagen fibril sizes.

METHODS: Study Design: Female wildtype (WT, n=36), $Dcn^{flox/flox}$ (I-$Dcn^{-/-}$, n=36), $Bgn^{flox/flox}$ (I-$Bgn^{-/-}$, n=36), and compound $Dcn^{flow/flox}/Bgn^{flox/flox}$ (I-$Dcn^{-/-}/Bgn^{-/-}$, n=36) mice with a tamoxifen (TM) inducible Cre, (B6.129-Gt(ROSA)26Sortm1(cre/ERT2)Tyj/J, Jackson Labs) were utilized (IACUC approved). At maturity (120 days), mice underwent bilateral patellar tendon injury surgery as described.[1,3] Following surgery, Cre excision of the conditional alleles was induced via two consecutive daily IP injections of TM (2 mg/40g body weight). WT mice received TM injections at 120 days and were divided between the uninjured control group, which was sacrificed at 150 days, and injured groups sacrificed at 3 or 6 weeks postinjury. Mice from inducible knockdown genotypes underwent surgery and were evenly divided between Cre-induction during the early proliferative period (TM injections beginning at 5 days post injury, termed TM5) or during the remodeling period (TM injections beginning at 21 days post injury, termed TM21). TM5 animals were sacrificed at 3 or 6 weeks postinjury, while TM21 mice were sacrificed at 6 weeks postinjury (n=16/genotype/induction timepoint/sacrifice timepoint). Gene: Injured patellar tendons were isolated for RNA extraction and cDNA reverse transcription. Pre-amplified cDNA was loaded into a Fluidigm 96.96 Dynamic Array with Taqman assays to probe expression levels of 96 target genes relevant for tendon healing (n=4/genotype/sacrifice timepoint). Histology: Whole knees were fixed, decalcified, paraffin embedded, sectioned in the transverse plane, and stained with toluidine blue (n=4/genotype/sacrifice timepoint). Images were used to quantify scarred area within the injured patellar tendons. Transmission Electron Microscopy (TEM): For TEM, injured patellar tendons were fixed, embedded in epon, sectioned at 85 nm, stained, and digitally imaged at 60,000x. Collagen fibril distributions were quantified from images captured within the healing region (n=4/genotype/sacrifice timepoint). Statistics: For gene expression and scar area, comparisons were made at each induction-sacrifice timepoint combination using three separate one-way ANOVAs with Tukey post-hoc tests (significance at $p \leq 0.05$; trends at $p \leq 0.1$). For collagen fibril size distributions, comparisons were made at each induction-sacrifice timepoint combination with Kolmogorov–Smirnov tests (significance at $p \leq 0.05$).

RESULTS: All knockdown groups demonstrated expected decreases in the targeted genes (Fig 1A-B). Further analysis at 3 weeks postinjury revealed increased expression of genes associated with matrix remodeling, inflammation, and activated fibroblasts in the TM5 I-$Dcn^{-/-}/Bgn^{-/-}$ group relative to all other groups (Table 1). At 6 weeks postinjury, the TM5 I-$Bgn^{-/-}$ and I-$Dcn^{-/-}/Bgn^{-/-}$ groups displayed increased expression of matrix remodeling genes, including Adamts5, Fbn1, Loxl2, and Mmp2, relative to the TM5 WT and I-$Dcn^{-/-}$ groups. In the TM21 groups, the increased expression of similar matrix remodeling genes was maintained in I-$Bgn^{-/-}$ tendons but not I-$Dcn^{-/-}/Bgn^{-/-}$ tendons. While there were no differences in relative scar area between groups (data not shown), fibril size distributions were significantly different between all groups compared (Fig 2A-C).

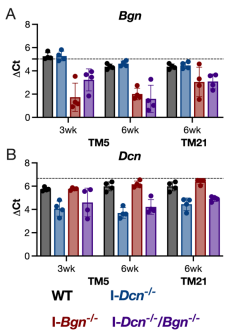

Figure 1. A) *Bgn* and B) *Dcn* demonstrated expected decreases in expression when targeted for knockdown with at least a trending difference relative to other groups, except for WT vs I-$Dcn^{-/-}/Bgn^{-/-}$ at TM5-3wk ($p = 0.15$). ΔCt was calculated by subtracting the gene Ct from average housekeeping Ct (Abl1 and Rps17).

DISCUSSION: Consistent with our hypothesis, the I-$Bgn^{-/-}$ and I-$Dcn^{-/-}/Bgn^{-/-}$ tendons demonstrated increased expression of matrix remodeling genes relative to WT and I-$Dcn^{-/-}$ tendons at 6 weeks postinjury, which is consistent with improved mechanical properties in these groups.[4,5] Interestingly, increased expression of these genes depended on induction timepoint, as this was observed in both I-$Bgn^{-/-}$ and I-$Dcn^{-/-}/Bgn^{-/-}$ groups at TM5 but only in the I-$Bgn^{-/-}$ group at TM21. This suggests that *Dcn* has a more prominent role between 5 and 21 days postinjury. Contrary to our hypothesis, we did not observe reduced scarred matrix nor a return to an uninjured distribution of collagen fibrils in I-$Bgn^{-/-}$ and I-$Dcn^{-/-}/Bgn^{-/-}$ tendons. While the I-$Bgn^{-/-}$ group exhibited a narrower distribution of fibrils at TM5 compared to WT, the lack of difference at TM21 suggests that the improved mechanical properties previously observed at both TM5 and TM21 are not due to changes in collagen fibril size distributions. Instead, we speculate that superior healing in these groups is due to changes in the non-collagenous tendon matrix, which then influences matrix synthesis, deposition, and organization. This is supported by observed increases in gene expression for non-collagenous matrix components and matrix remodeling proteins in these groups.

SIGNIFICANCE: This study investigated the roles of the SLRPs decorin and biglycan during the early proliferative and remodeling phases of tendon healing. This data indicates that *Bgn* knockdown increases non-collagenous matrix and matrix remodeling gene expression following injury, which is consistent with improved mechanical properties previously observed with knockdown of *Bgn* in healing tendons.

ACKNOWLEDGEMENTS: We acknowledge financial support from NIH/NIAMS (R01AR068057, T32AR007132, P30AR069619), and contributions from Jaclyn Carlson, Michael DiStefano, and Ryan Leiphart.

REFERENCES: 1. Dunkman *et al.*, *Ann. Biomed. Eng.*, 2014. 2. Dourte *et al.*, *J. Orthop. Res.*, 2013. 3. Dunkman *et al., Matrix Biol.* , 2014. 4. Fung *et al.*, ORS Annual Meeting, 2020. 5. Leahy *et al.*, ORS Annual Meeting, 2020.

TM5-3wk

Up / Down	WT	I-$Dcn^{-/-}$	I-$Bgn^{-/-}$	I-$Dcn^{-/-}/Bgn^{-/-}$
WT		Lum, Mmp13	Eln	Fbn1, Mmp3, Ptk2, Igf1, Adgre1
I-$Dcn^{-/-}$	Pdgfb			Fbn1, Tnc, Loxl2, Col4, Ptk2, Pdgfb, Pge2, Col4, Adgre1
I-$Bgn^{-/-}$	Cd146, Vegfb, Pdgfb, Egr1	Lum, Cd146, Col8		Loxl2, Col44, Cd146, Acta2, Ptk2, Pge2, Col8, Adgre1, Cox2
I-$Dcn^{-/-}/Bgn^{-/-}$				

TM5-6wk

Up / Down	WT	I-$Dcn^{-/-}$	I-$Bgn^{-/-}$	I-$Dcn^{-/-}/Bgn^{-/-}$
WT		Col1a2, Ptk2, Igf1, Tgfb3	Fbn1, Fbn2, Eln, Aspn, Loxl2, Mmp2, Itgb3, Igf1, Pge2, Cdkn1a	Fn1, Pg4, Loxl2, Mmp2, Itgb3, Igf1, Pge2, Pdgfb, Tgfb3, Cdkn1a
I-$Dcn^{-/-}$			Aspn, Adamts5, Loxl2, Itgb3, Cdkn1a	Adamts5, Loxl2, Itgb3
I-$Bgn^{-/-}$				
I-$Dcn^{-/-}/Bgn^{-/-}$				

TM21-6wk

Up / Down	WT	I-$Dcn^{-/-}$	I-$Bgn^{-/-}$	I-$Dcn^{-/-}/Bgn^{-/-}$
WT		Tgfb3	Col1a2, Thbs4, Fmod, Tnc, Col4, Bmp2, Igf1, Pdgfa, Tgfb3, Pdgfb, Cdkn1a	Aspn, Eln, Col4
I-$Dcn^{-/-}$			Thbs4, Tnc, Mmp2, Mmp3, Tnmd, Itga11, Col4, Cdkn1a	Aspn
I-$Bgn^{-/-}$				
I-$Dcn^{-/-}/Bgn^{-/-}$	Col1a1	Col1a1, Pgdfa	Col1a1, Col1a2, Col11a1, Thbs4, Fmod, Tnc, Mmp2, Mmp3, Tnmd, Itga11, Spp1, Pdgfa, Tgfb3, Cdkn1a	

Table 1. Gene expression summary table. Genes listed are significantly increased in the column group relative to the row group.

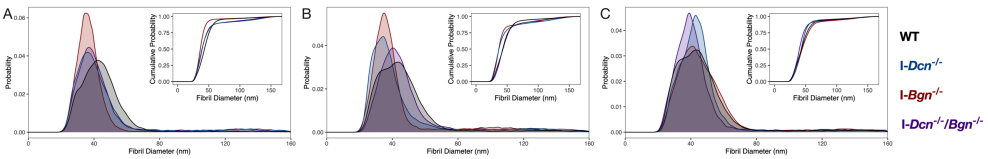

Figure 2. Probability density and cumulative distributions (insets) plots for A) TM5-3wk, B) TM5-6wk, and C) TM21-6wk.

Collagen V Knockdown Alters Collagen Fibril Size, but Not Mechanics, in Mature Female Murine Tendons

Ryan J Leiphart[1], Stephanie N Weiss[1], Jaclyn A Carlson[1], Patrick L Paglia-Garcés[1], Louis J Soslowsky[1]
[1]McKay Orthopedic Research Laboratory, University of Pennsylvania, Philadelphia, PA

Disclosures: RJ Leiphart (N), SN Weiss (N), JA Carlson (N), PL Paglia-Garcés (N), LJ Soslowsky (N)

INTRODUCTION: Collagen V is a critical tendon matrix regulator that controls collagen I fibril size [1], and collagen V knockdown during tendon homeostasis increased the viscoelasticity of male murine tendons [2]. However, tendons display sex-dependent gene expression changes in response to collagen V knockdown [3], and the effect of this knockdown and differential gene expression on female murine tendon properties remains unknown. Therefore, the objective of this study was to define the effect of collagen V knockdown on mature female murine patellar tendon mechanical properties and collagen fibril size. Based on observed increases in matrix expression following collagen V knockdown [3], we hypothesized that collagen V knockdown would increase the mechanical properties and collagen fibril size of female murine patellar tendons.

METHODS: *Animals* – Female wild-type (WT) and bitransgenic *Col5a1*$^{flox/+}$ and *Col5a1*$^{flox/flox}$ mice with *ROSA26-CreER*^{T2} were used in this study (IACUC approved). At 120 days old, mice received 3 consecutive daily tamoxifen (TM) injections (4mg/40g body weight) for Cre-mediated excision of floxed *Col5a1* alleles, resulting in I-*Col5a1*$^{+/-}$ and I-*Col5a1*$^{-/-}$ genotypes. Mice were sacrificed 30 days post-TM injections. Hindlimbs were harvested, and patellar tendons were isolated and prepared for mechanical testing (n=15/genotype) or transmission electron microscopy (TEM, n=4/genotype) as described [4]. *Mechanical Testing* – Tendons were immersed in a 37ºC 1x PBS bath and loaded into an Instron 5848. Tendons underwent the following viscoelastic testing protocol: preconditioning, 10 min stress relaxations at 3, 4, and 5% strain, each followed by 10 cycle frequency sweeps at 0.1, 1, 5, and 10Hz, and a ramp-to-failure. Percent relaxation, dynamic modulus, and phase shift were computed from each stress relaxation and frequency sweep. Stiffness, max load, modulus, and max stress were measured from ramp-to-failure tests. *Collagen Fibril Imaging* – Following fixation and processing, tendons were sectioned at ~90nm and imaged with a JEOL 1400 TEM. 10 regions were analyzed per tendon. Collagen fibril diameter was measured across the fibril minor axis with BIOQUANT. *Statistics* – One-way ANOVAs with Tukey post-hoc tests were used to compare mechanical properties across genotypes. Collagen fibril diameter distributions from each genotype were compared against those of the other genotypes using Kolmogorov-Smirnov tests. Significance was set at $p \leq 0.05$ and trends at $p \leq 0.1$.

RESULTS: No differences in any measured mechanical properties were observed across WT and knockdown genotypes; this included stiffness (Fig 1A), max load (Fig 1B), modulus (Fig 1C), max stress (Fig 1D), percent relaxation, dynamic modulus, and phase shift (data not shown). Conversely, collagen fibril size distributions were significantly different across all genotypes (Fig 2, $p<0.0001$). WT tendons displayed a characteristic bimodal fibril size distribution (Q1: 74.3nm, Q2: 111.6nm, Q3: 139.0nm). I-*Col5a1*$^{+/-}$ tendons exhibited a larger spread in fibril size, with increased proportion of small (<70nm) and large (>160nm) diameter fibrils (Q1: 65.7nm, Q2: 103.1nm, Q3: 137.2nm). I-*Col5a1*$^{-/-}$ tendons contained an increased proportion of fibrils between 100-140nm in diameter (Q1: 80.1nm, Q2: 114.3nm, Q3: 138.2nm).

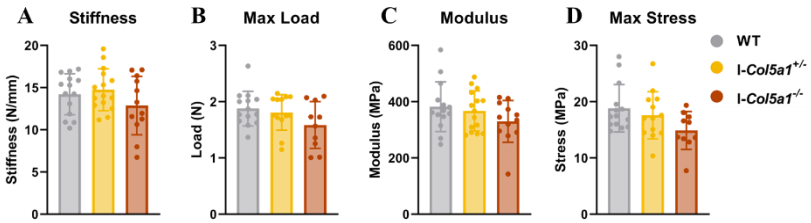

Figure 1. Collagen V knockdown does not impact female tendon mechanical properties. No differences in stiffness (A), max load (B), modulus (C), or max stress (D) were observed across genotypes.

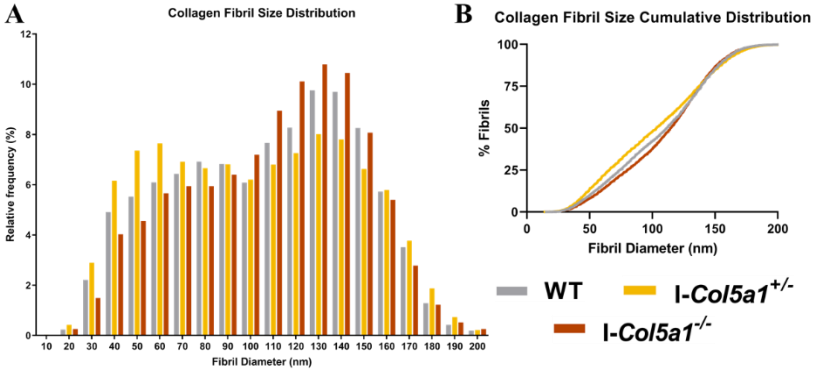

Figure 2. Collagen V knockdown alters collagen fibril size in an allele-dependent manner. WT tendon fibrils demonstrate a characteristic bimodal size distribution. I-*Col5a1*$^{+/-}$ tendons had a higher proportion of small (<70nm) and large (>160nm) diameter fibrils. I-*Col5a1*$^{-/-}$ tendons displayed a larger proportion of intermediately sized fibrils (100-140nm). All distributions were significantly different from each other ($p<0.0001$).

DISCUSSION: Contrary to our hypothesis, acute knockdown of collagen V in mature female mice did not significantly alter patellar tendon mechanical properties. Despite the lack of mechanical changes, collagen V knockdown resulted in allele-dependent changes to collagen fibril size distribution. Taken together, these results provide key insights into the sex-linked role of collagen V in homeostatic tendon function. While collagen V knockdown in mature female murine tendons did not impact mechanical properties as shown here, collagen V knockdown did lead to increased viscoelasticity in mature male tendons [2]. Both sexes experienced changes in collagen fibril size in response to collagen V knockdown. This suggests that homeostatic female tendon function is less sensitive to collagen V presence than male tendon function. The decreased sensitivity to collagen V presence in female tendons may be due to observed increases in matrix synthesis expression in response to collagen V knockdown [3]. A limitation of this study is the global nature of the *Col5a1* knockdown model used. While this may lead to confounding effects in other tissues, the short knockdown window employed here likely minimized these effects. Future studies will assess the histological properties of knockdown tendons to further delineate the sex-dependent response to collagen V knockdown.

SIGNIFICANCE: This work demonstrates a sex-linked role of collagen V in dictating homeostatic tendon function. Understanding this sex-dependent role can inform therapeutics that treat collagen V-associated clinical disorders.

REFERENCES: [1] Wenstrup RJ et al. *J Biol Chem*. 2011. [2] Leiphart RJ et al. *ORS Annual Meeting*. 2020. [3] Leiphart RJ et al. *ORS Annual Meeting*. 2021. [4] Dunkmann AA et al. *Matrix Biol*. 2013.

ACKNOWLEDGEMENTS: This work was supported by the NIH (R01AR065995, P30AR069619) and the NSF GRFP.

Regional FDL Tendon Development Involves Differential Pericellular Matrix Expression and Presence

Ryan J Leiphart[1], Stephanie N Weiss[1], Nathaniel A Dyment[1], Louis J Soslowsky[1]
[1]McKay Orthopedic Research Laboratory, University of Pennsylvania, Philadelphia, PA

Disclosures: RJ Leiphart (N), SN Weiss (N), NA Dyment (N), LJ Soslowsky (N)

INTRODUCTION: Tendon requires highly aligned collagen I fibrils to aid in mechanical strength in response to tensile loading. Regions of tendon that wrap around bones or joints, however, experience additional compressive loading and display a complex, fibrocartilaginous tissue phenotype [1]. Fibrocartilage and resident chondrogenic cells rely heavily on the collagen VI-rich pericellular matrix (PCM) for proper mechanosensation and homeostasis [2]. While the fibrocartilage matrix within wrap-around tendon regions has been characterized [3], the development of this unique tissue region and its PCM content remains unknown. Therefore, the objective of this study was to define differential PCM expression and presence within the highly aligned (tensile) tendon matrix and the wrap-around (compressive) fibrocartilage matrix during murine FDL tendon development. We hypothesized that PCM expression and synthesis is increased in the compressive region compared to the tensile region as early as two-weeks postnatally due to compressive joint loads from ambulation at this age.

METHODS: *Animals* – Wild-type P7 (n=9), P14 (n=7/sex) and P21 (n=7/sex) mice were used in this study (IACUC approved). At sacrifice, mouse hindlimbs were harvested, fixed in 4% RNAse-clean PFA for 3hr, then embedded and flash frozen in OCT. Embedded limbs were cryosectioned at 20μm for gene expression or at 8μm for histological staining. *Gene Expression* – Tensile and compressive regions of sectioned FDL tendon were microdissected and separated using 25G needles. Regional samples were digested with proteinase K, and RNA was extracted with Zymo Quick-RNA MicroPrep kits. cDNA was reverse transcribed and preamplified for 15 cycles with *Col6a(1-3)*, *Bgn*, and *Abl1* Taqman assays. RT-qPCR was performed on preamplified cDNA for those target genes. ΔCt values for each gene were calculated based on corresponding *Abl1* Ct values. *Histology* – After fixation, samples were decalcified with EDTA for 4-5 days prior to embedding and sectioning. Sections were stained with rabbit anti-collagen VI antibody (Fitzgerald, 70R-CR009x) and Hoechst nuclear stain prior to being imaged on a Zeiss Axio Scan.Z1. The tensile and compressive tendon regions were segmented, and mean antibody intensity was quantified for each region using FIJI. *Statistics* – Paired t-tests were used to compare ΔCt values for measured genes and mean staining intensity between the tensile and compressive region. Significance was set at $p \leq 0.05$ and trends at $p \leq 0.1$.

RESULTS: In P7 FDL tendons, the compressive region showed increased expression of *Col6a1*, with trending increases in *Col6a2* and *Bgn*, compared to the tensile region (Fig 1). At P14, the compressive region exhibited increased expression of all measured *Col6* genes and of *Bgn* compared to that of the tensile region. At P21, *Col6a3* and *Bgn* had trending expression increases in the compressive region compared to the tensile region. Quantification of collagen VI antibody staining revealed no regional differences in P7 FDL tendons (Fig 2). However, mean staining intensity was increased in the compressive region compared to the tensile region at P14 and P21.

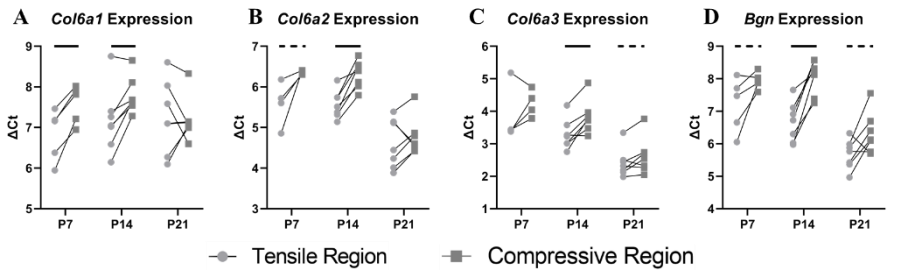

Figure 1. Region-dependent PCM gene expression peaks at P14. Expression of *Col6* genes (A-C) and of *Bgn* (D) was higher in the compressive region compared to the tensile region by P14. Most of these regional differences were not present at P21. Solid lines denote $p \leq 0.05$, dotted lines denote $p \leq 0.1$.

DISCUSSION: Results demonstrate that regional differences in PCM begin at early postnatal ages in the FDL tendon. The tendon PCM is comprised of collagen VI α-chains [4], and evidence suggests that biglycan helps organize the tendon PCM [5]. While the compressive region exhibited some increases in PCM gene expression compared to the tensile region at P7, this increased expression was consistently observed across all measured genes by P14. This expression pattern was supported by elevated PCM content in the compressive region at P14, which persisted at P21. Supporting our hypothesis, this result suggests that increased PCM expression and synthesis in the compressive region is driven by complex joint loads during murine gait. Mice begin walking quickly by two weeks of age [6], which would lead to increased joint flexion and loading on wrap-around tendons. Tendon cells respond to these forces by producing a fibrocartilaginous, GAG-rich matrix [7] with thickened PCM staining (Fig 2).

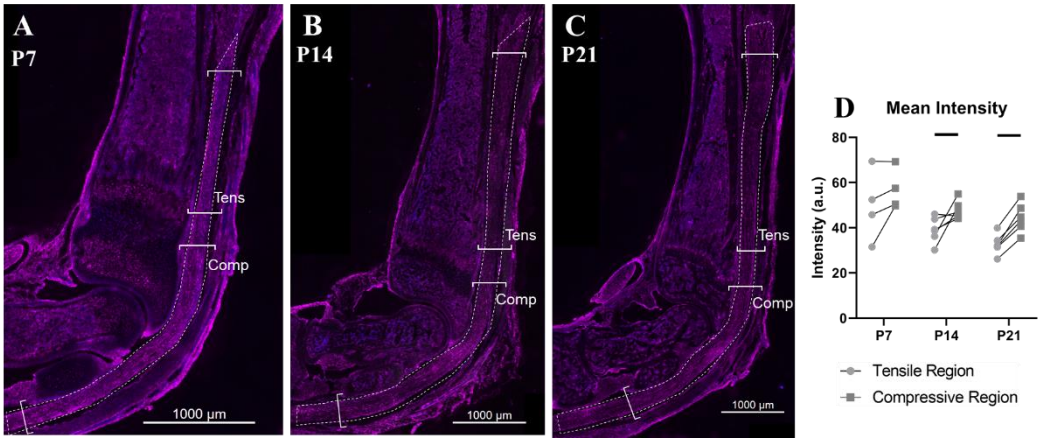

Figure 2. Region-dependent PCM presence is apparent at P14. Collagen VI staining (pink) reveals no differences in intensity between the tensile (Tens) and compressive (Comp) regions of the FDL tendon at P7 (A). By P14 (B), the compressive region contains higher intensity staining compared to the tensile region, which persists at P21 (C). Signal intensity quantification shows that these changes are significant (D). Solid lines denote $p \leq 0.05$.

As a result, the tendon PCM is likely a critical regulator of tendon cell phenotype. A limitation of this study is the inability to precisely define tensile and compressive tendon regions, as there are likely no regions that experience purely compressive or tensile loading. However, prior studies demonstrate that regional differences in wrap-around tendons are exacerbated by compressive loading [7,8], supporting our definitions of tensile and compressive tendon regions. Anatomical markers were used to segment these regions, making them consistent across samples and age groups. Future work will analyze the differential response of these FDL tendon regions to knockout of PCM molecules.

SIGNIFICANCE: This work defines temporal regional development of the PCM within the murine FDL tendon. Understanding the differential development of these tendon regions provides insight into how tendon cells respond to physical cues, which is critical for treatment paradigms.

REFERENCES: [1] Benjamin M et al. *J Anat*. 1998. [2] Sanchez-Adams J et al. *J Orthop Res*. 2013. [3] Perez-Castro AV et al. *J Orthop Res*. 1999. [4] Ritty TM et al. *Structure*. 2003. [5] Wiberg C et al. *J Biol Chem*. 2002. [6] Clarke KA et al. *Physiol. Behav*. 2001. [7] Evanko SP et al. *Arch Biochem Biophys*. 1993. [8] Malaviya P et al. *J Orthop Res*. 2000. **ACKNOWLEDGEMENTS:** This work was supported by the NIH (P30AR069619) and the NSF GRFP.

Knockdown of Decorin and Biglycan Immediately Following Tendon Injury Significantly Alters Gene Expression and Fibril Morphology, with Minimal Effects on Mechanical Properties

Joseph B. Newton[1], Stephanie N. Weiss[1], Christelle Darrieutort-Laffite[1,2], Courtney A. Nuss[1], David E. Birk[3], Louis J. Soslowsky[1]
[1]McKay Orthopaedic Research Laboratory, University of Pennsylvania, Philadelphia, PA, [2]Rheumatology Department, Nantes University Hospital, France
[3]Department of Molecular Pharmacology and Physiology, University of South Florida, Tampa, FL
josebr@seas.upenn.edu

Disclosures: Joseph B. Newton(N), Stephanie N. Weiss(N), Christelle Darrieutort-Laffite(N), Courtney Nuss(N), David E. Birk(N), Louis J. Soslowsky(N)

INTRODUCTION: Tendon consists of highly organized collagen fibrils with small leucine rich proteoglycans (SLRPs) bound to the fibril surface. Two of these SLRPs, decorin (Dcn) and biglycan (Bgn) play important roles throughout tendon growth, aging, and repair as regulators of fibrillogenesis and matrix assembly [1]. Biglycan is highly expressed in the immediate response to tendon injury and early stages of tendon growth, but decreases dramatically during remodeling and in mature tendons, while decorin is present throughout these processes [2]. However, the roles of decorin and biglycan in the initial injury response in aged tendons are unknown. Therefore, the objective of this study is to evaluate the differential roles of decorin and biglycan through their knockdown at the time of injury in aged mice. We hypothesized that induced knockdown of decorin and biglycan expression, individually and in a double knockdown, would impair the healing response compared to wild type mice leading to reduced improvement in tendon mechanical properties post injury, altered gene expression profiles, and changes in collagen fibril diameter distributions. As the predominant SLRP in tendon, we hypothesized that knockdown of decorin would result in greater impairment as biglycan expression is minimal in mature tendons.

METHODS: Study Design: Female *Dcn*$^{+/+}$/*Bgn*$^{+/+}$ control (WT, n=48), *Dcn*$^{flox/flox}$ (I-*Dcn*$^{-/-}$, n=32), *Bgn*$^{flox/flox}$ (I-*Bgn*$^{-/-}$, n=32), and compound *Dcn*$^{flox/flox}$/*Bgn*$^{flox/flox}$ (I-*Dcn*$^{-/-}$/*Bgn*$^{-/-}$, n=32) mice with a tamoxifen inducible Cre (B6.129-Gt(ROSA)26Sortm1(cre/ERT2)Tyj/J, Jackson Labs) were utilized [3] (IACUC approved). At 300 days old, Cre excision of conditional alleles was induced in all mice via two (injured mice) or three (uninjured mice) consecutive daily IP injections of tamoxifen. WT mice (n=16) were designated as uninjured controls and remaining mice were divided into 3- or 6-week post-injury groups to represent the early and later remodeling healing phases (n=16/genotype/time point). At time of induction, mice in injury groups underwent bilateral patellar tendon injury surgery and were sacrificed 1-, 3- or 6-weeks later. Uninjured groups were sacrificed at 330 days old. Mechanical Testing Protocol: The patellar tendon-bone complex from one limb of each animal in the 3- and 6-week post-injury groups was dissected and prepared for mechanical testing (n=10-14/genotype/time point) [4]. Tendons were subjected to a testing protocol: preconditioning, stress relaxations at 3, 4, and 5% strains, and a quasi-static ramp to failure. Tendon elastic mechanical properties were calculated from the ramp to failure test and stain lines were used for optical strain tracking. Percent relaxation was quantified for each stress-relaxation. Transmission Electron Microscopy (TEM): For TEM, patellar tendons from animals in the 6-week post-injury group were fixed, embedded in epon, sectioned at 75nm, and imaged at 60,000x. Collagen fibril distributions were quantified from images in the healing region (n=4/genotype). Gene: Injured patellar tendons from animals in the 1-, 3-, and 6-weeks post injury groups were isolated for RNA extraction and cDNA reverse transcription. Pre-amplified cDNA was loaded into a Fluidigm 96.96 Dynamic Array with Taqman assays to probe expression levels of 96 target genes relevant for tendon healing (n=4/genotype/time point). Statistics: For mechanics, one-way ANOVAs with Bonferroni corrections were conducted for 3- and 6-week post-injury groups. For gene expression, the same tests were conducted for 1-, 3-, and 6-week post injury groups. Fibril diameter distributions were compared using Kolmogorov-Smirnov tests. Significance was set at $p \leq 0.05$.

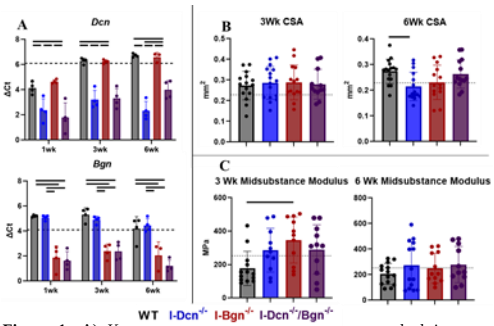

Figure 1: A) Knockdown of decorin and biglycan resulted in a significant reduction in expression levels. B) A significant decrease in cross-sectional area (CSA) was found comparing I-Dcn$^{-/-}$ to WT tendons 6-weeks post-injury. C) A significant increase in midsubstance modulus was found in I-Bgn$^{-/-}$ tendons compared to WT at 3-weeks post-injury. Bars indicate significance at $p \leq 0.05$. Dashed line denotes uninjured WT values.

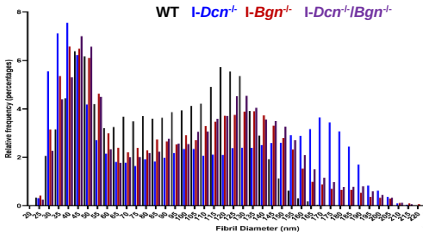

Figure 2: Relative frequency of fibril diameter taken from TEM.

RESULTS: Decorin and biglycan expression showed efficient knockdown (Fig 1A). Tendon cross-sectional area was decreased in the I-*Dcn*$^{-/-}$ group vs WT (Fig 1B). Midsubstance modulus was increased in I-*Bgn*$^{-/-}$ vs WT (Fig 1C). No differences were found in max stress and percent relaxation (not shown). Fibril distributions were different between all groups at 6-weeks post-injury (Fig 2). At 1-week post-injury, I-*Bgn*$^{-/-}$ had increased expression of genes related to collagen and non-collagenous matrix synthesis, inflammation, and cell-ECM interactions compared to WT tendons (Table 1). 3- and 6-weeks post-injury reveals I-*Dcn*$^{-/-}$ tendons have reduced expression of genes related to collagen synthesis, non-collagenous matrix synthesis, matrix remodeling, inflammation, and cell-ECM interactions compared to WT, I-*Bgn*$^{-/-}$ and I-*Dcn*$^{-/-}$/*Bgn*$^{-/-}$ groups (Table 1).

1-Wk

UP / Down	WT	I-*Dcn*$^{-/-}$	I-*Bgn*$^{-/-}$	I-*Dcn*$^{-/-}$/*Bgn*$^{-/-}$
WT			*Col1a2, Postn, Ly6a, Itgb1, Ltbp1, Ly6a, Ltbp1*	*TNF, Tlr2, P2x7*
I-*Dcn*$^{-/-}$	*Col2a1*		*Col1a1*	
I-*Bgn*$^{-/-}$				*TNF, P2x7*
I-*Dcn*$^{-/-}$/*Bgn*$^{-/-}$	*Col2a1*			

3-Wk

UP / Down	WT	I-*Dcn*$^{-/-}$	I-*Bgn*$^{-/-}$	I-*Dcn*$^{-/-}$/*Bgn*$^{-/-}$
WT		*Elastin*		
I-*Dcn*$^{-/-}$	*Col12a1, Kera, Fbn2, Fbln4, Thbs2, Tnc*		*Col12a1, Thbs4, Tnc, Tnxb, MMP3, Mkx, Itgb1*	*Col1a2, Col11a1, Col12a1, Kera, Fbn2, Thbs2, Tnc, Tnxb, MMP14, Sox9, Itgb1, Pge2, Igf1*
I-*Bgn*$^{-/-}$	*IL10*	*IL10*		
I-*Dcn*$^{-/-}$/*Bgn*$^{-/-}$	*Ly6a*	*Timp3*	*Ltbp1*	

6-Wk

UP / Down	WT	I-*Dcn*$^{-/-}$	I-*Bgn*$^{-/-}$	I-*Dcn*$^{-/-}$/*Bgn*$^{-/-}$
WT		*Col3a1*		*Ccl5*
I-*Dcn*$^{-/-}$	*Fmod, Kera, Timp3, Runx2, Mkx*		*Fmod, Timp3, Mkx*	*Thbs4, Timp3, Mkx, Ctgf, Bmp2*
I-*Bgn*$^{-/-}$				
I-*Dcn*$^{-/-}$/*Bgn*$^{-/-}$				

Table 1: Gene expression summary table. Genes listed are significantly increased in the column group relative to the row group.

DISCUSSION: Our study supports the differential roles of decorin and biglycan throughout healing. At 1-week, most changes in gene expression were found in I-*Bgn*$^{-/-}$ tendons suggesting that biglycan plays a critical role during the inflammatory phase of healing. [2]. At 3-weeks, gene expression changes were found in I-*Dcn*$^{-/-}$ tendons that were not fully maintained at 6-weeks post-injury. Decorin and biglycan have been shown to be involved in matrix assembly, inflammation, and growth factor activity during healing [4,5]. Both single and double knockdown of biglycan and decorin led to tendons with a smaller fibril diameter 6-week post injury, further highlighting the role of these SLRPs in fibrillogenesis [6]. Surprisingly, these changes were not reflected in mechanical properties, with only an increase in midsubstance modulus 3-weeks post-injury in I-*Bgn*$^{-/-}$ tendons vs WT. Contrary to our hypotheses, knockdown at the time of injury did not lead to differences in mechanical properties 6-weeks post-injury. These results may suggest a more limited role of decorin and biglycan during later stages of healing in aged mice. Future work is necessary to elucidate the roles of decorin and biglycan at the later stages of healing.

SIGNIFICANCE: This study highlights the differential roles of biglycan and decorin in gene expression and fibril structure during healing in aged mice and suggests that biglycan has a larger role in the early phases of healing, while decorin is more pronounced at 3- weeks post injury.

ACKNOWLEDGEMENTS: We acknowledge financial support from NIH/NIAMS (R01AR068057 and P30AR069619).

REFERENCES: [1] Chen et al., *FEBS J*, 280, 2013. [2] Dunkman et al., *Ann Biomed Eng*, 42, 2014. [3] Robinson et al., *Matrix Biol*, 64, 2017. [4] Connizzo et al., *J Biomech Eng*, 135, 2013. [5] Iozzo et al., *J Biol Chem, 286*, 2011. [6] Hildebrand et al., *Biochem J*, 302, 1994.

Scleraxis Targeted Deletion of Collagen XI Disrupts Mouse Patellar Tendon Structure During Postnatal Development

Matthew K. Stein[1], Snehal S. Shetye[1], Courtney A. Nuss[1], Ashley K. Fung[1], Jaclyn A. Carlson[1], Stephanie N. Weiss[1], Jordan S. Cohen[1], Nathaniel A. Dyment[1], Louis J. Soslowsky[1]

[1]McKay Orthopaedic Research Lab, University of Pennsylvania, Philadelphia, PA

Author Disclosures: Matthew K. Stein (N), Snehal S. Shetye (N), Courtney A. Nuss (N), Ashley K. Fung (N), Jaclyn A. Carlson (N), Stephanie N. Weiss (N), Jordan S. Cohen (N), Nathaniel A. Dyment (N), Louis J. Soslowsky (N)

INTRODUCTION: Type II Stickler Syndrome is caused by mutations in the COL11A1 gene and manifests with abnormalities in facial morphology, ocular development, and joint problems including hypermobility and early arthritis [1]. Beyond its role in chondrogenesis, collagen XI plays a role in tendon development related to its co-assembly with collagen I and II during heterotypic fibril formation, and targeted collagen XI knockout in adult tendons results in reduced fibril number and aberrant structure [2]. Collagen XI is most highly expressed during tendon development, yet the effects of collagen XI knockdown on tendon structure in early postnatal development remains unknown. Therefore, the objective of this study was to define the role of collagen XI in tendon organization and structure, focusing on its effects on nuclear orientation, patellar tendon length and thickness, and fibril diameter throughout postnatal development. We hypothesized that tendon-targeted collagen XI knockout mice would have increased patellar tendon length with greater nuclear dispersion and decreased fibril diameter when compared to control mice.

METHODS: Tendon-targeted ScxCre *Col11a1*$^{flox/flox}$ (called NULL for this study), ScxCre, *Col11a1*$^{flox/wt}$ (called HET), and Cre- littermate control (called CTRL) mice were used in this study (IACUC approved). Knee joints and patellar tendons were isolated from mice at postnatal day (P) 0, 10, 20, and 30 for histology (n=4/group) and transmission electron microscopy (TEM; n=4/group). Histology: Knees were fixed in formalin, embedded in optical cutting temperature compound, and cryosectioned in the sagittal plane [3]. Sections were stained with Hoechst 33342 to evaluate nuclear organization followed by toluidine blue to assess tendon morphology. Dispersion was calculated in ImageJ, which fit a Gaussian function to a histogram of the direction of the patellar tendon nuclei to determine the standard deviation of this distribution. Tendon length (from patellar origin to tibial insertion) and thickness (averaged over 10 locations across the tendon) were evaluated. Nuclear dispersion, length, and thickness were compared across ages and genotypes using 2-way ANOVA tests with Bonferroni post-hoc corrections. TEM: Samples were prepared as described [4,5]. Histograms pooling fibril diameters into 10 nm bins and the ensuing distributions were compared using Kolmogorov-Smirnov tests. For all analyses, significance was set at $p \leq 0.05$.

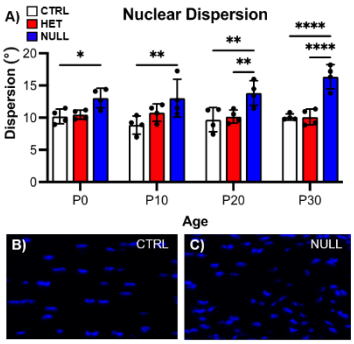

Figure 1: A) Nuclear dispersion was increased in ScxCre;*Col11a1*$^{f/f}$ (NULL) tendons compared to HET and Cre- littermates (CTRL). (*p≤ 0.05; **p≤ 0.005; ****p≤ 0.0001) B) Representatives images of nuclear organization in P30 patellar tendons show increased dispersion in the C) NULL group.

RESULTS: con

Patellar tendon length was also assessed at all ages. There were no differences in patellar tendon length across genotypes at P0 and P10. However, by P20, NULL patellar tendons were longer than HET and CTRL tendons ($p<0.05$) (**Figure 2A**). These findings persisted at P30, with the difference in length increasing to 1.45 mm between NULL and CTRL mice at this age (**Figure 2B,C**). In contrast, patellar tendon thickness was not significantly different across genotypes at any age (data not shown).

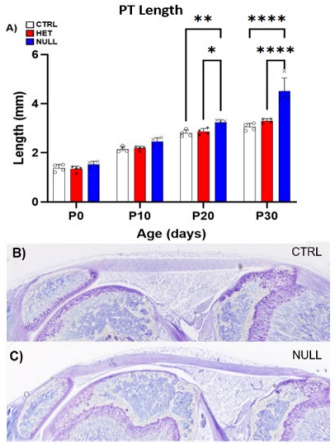

Figure 2: A) There were no differences in length at P0 and P10; however, patellar tendons were significantly longer in ScxCre;*Col11a1*$^{f/f}$ (NULL) mice than HET and CTRL. (*p≤ 0.05; **p≤ 0.005; ****p≤ 0.001) B) Representative images at P30 demonstrate increased length in C) NULL tendons.

TEM was performed at all ages to evaluate the effect of tendon-targeted collagen XI knockout on fibril diameter. At P0, fibril diameter distribution appeared similar across genotypes (**Figure 3A**). By P10, the HET and NULL groups developed greater variability in fibril diameters with an increase in the number of large fibrils ($p<0.001$) (**Figure 3B**). At P30, the magnitude of this finding increased with more large fibrils seen in the HET and NULL groups ($p<0.001$) (**Figure 3C**).

DISCUSSION: This study investigated the regulatory role of collagen XI during postnatal tendon development. Overall, our results demonstrated that collagen XI deficiency severely disrupts tendon structure resulting in nuclear disorganization, altered length, and altered fibril diameter distribution. The increased nuclear dispersion (NULL vs. CTRL) might indicate substantial loss in organization of underlying extracellular matrix. With development, collagen XI deficiency also resulted in increased patellar tendon length. Lengthening may be caused by accumulated tendon damage due to inability of the tendon to withstand the loading of daily activity. TEM analysis showed that NULL mice had overall greater fibril diameter compared to HET and CTRL littermates, with a greater range of fibril diameters. This may be related to disruptions in fibrillogenesis due to collagen XI knockdown. Prior work has shown that targeted collagen XI knockdown causes decreased cross-sectional area, stiffness, and failure load of the Achilles (ACH) and flexor digitorum longus (FDL) tendons in adult mice [6]. The histological and structural findings in this study at multiple developmental ages provide insight into the underlying causes of the weaker structural properties of adult tendons in NULL mice. Future work on the expression of tenogenic and chondrogenic markers during development may help to establish a mechanism driving the observed phenotype. Additionally, mechanical testing of tendons at these developmental time points will determine the timing of the mechanical weakening of tendons in NULL mice.

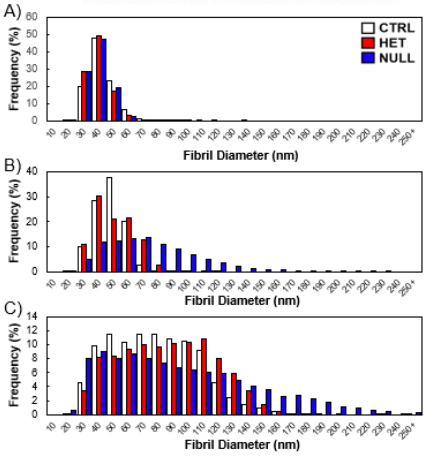

Figure 3: Histograms of patellar tendon fibril diameters across genotypes at A) P0 B) P10 and C) P30. At all timepoints, distributions for CTRL, HET, and NULL mice were statistically different ($p<0.001$).

SIGNIFICANCE: Results clearly highlight the critical role of collagen XI in tenogenesis and underscore the importance of further studying how this regulatory collagen influences the development and homeostasis of tendons despite being nearly absent in adult tendons.

REFERENCES: [1] Cattalini M et al., Pediatr Rheumatol Online J, 2015. [2] Wenstrup RJ et al. J Biol Chem, 2011. [3] Dyment NA et al. J Vis Exp, 2016. [4] Birk DE et al. Dev Dyn, 1995. [5] Birk DE et al. J Cell Biol, 1986 [6] Ye Y et al. Orthopaedic Research Society Annual Meeting, 2019.

ACKNOWLEDGMENTS: We thank Chet Friday and Michael DiStefano for their help with data analysis. This study was funded by NIH/NIAMS R01AR073231 and the Penn Center for Musculoskeletal Disorders (P30 AR069619).